PGJ/F-116(82)

National Uranium Resource Evaluation

CLIFTON QUADRANGLE ARIZONA AND NEW MEXICO

Bendix Field Engineering Corporation
Grand Junction, Colorado

Issue Date
May 1982

PREPARED FOR THE U.S. DEPARTMENT OF ENERGY
Assistant Secretary for Nuclear Energy
Grand Junction Area Office, Colorado

DISCLAIMER

This report is a result of work performed by Bendix Field Engineering Corporation, Operating Contractor for the U.S. Department of Energy, as part of the National Uranium Resource Evaluation. NURE is a program of the U.S. Department of Energy's Grand Junction, Colorado, Office to acquire and compile geologic and other information with which to assess the magnitude and distribution of uranium resources and to determine areas favorable for the occurrence of uranium in the United States.

Available from: Technical Library
Bendix Field Engineering Corporation
P.O. Box 1569
Grand Junction, CO 81502-1569

Telephone: (303) 242-8621, Ext. 278

Price per Microfiche Copy: $6.50

PGJ/F--116(82)

PGJ/F-116(82)

DE82 015181

NATIONAL URANIUM RESOURCE EVALUATION
CLIFTON QUADRANGLE
ARIZONA AND NEW MEXICO

David L. White and Mary Foster

BENDIX FIELD ENGINEERING CORPORATION
Grand Junction Operations
Grand Junction, Colorado 81502

March 1982

PREPARED FOR THE U.S. DEPARTMENT OF ENERGY
GRAND JUNCTION AREA OFFICE
UNDER CONTRACT NO. DE-AC07-76GJ01664

EAB

This is the final version of the subject-quadrangle evaluation report to be placed on open file. This report has not been edited. In some instances, reductions in the size of favorable areas on Plate 1 are not reflected in the text.

CONTENTS

CONTENTS (continued)

CONTENTS (continued)

ILLUSTRATIONS

ILLUSTRATIONS (continued)

ABSTRACT

The Clifton Quadrangle, Arizona and New Mexico, was evaluated to identify environments and delineate areas favorable for uranium deposits. The evaluation used criteria formulated for the National Uranium Resource Evaluation program. Evidence for the evaluation was based on surface studies, hydrogeochemical and stream-sediment reconnaissance, and aerial radiometric surveys. The quadrangle encompasses parts of three physiographic provinces: the Colorado Plateau, the transition zone, and the Basin and Range.

The one environment determined, during the present study, to be favorable for uranium deposits is the Whitewater Creek member of the Cooney tuff, which is favorable for magmatic-hydrothermal uranium deposits on the west side of the Bursum caldera. No other areas were favorable for uranium deposits in sandstone, limestone, volcanogenic, igneous, or metamorphic environments. The subsurface is unevaluated because of lack of information, as are areas where access is a constraint.

INTRODUCTION

PURPOSE

The Clifton Quadrangle, Arizona and New Mexico (Fig. 1), was evaluated to identify geologic environments and delineate areas that exhibit characteristics favorable for uranium deposits. Selection of a favorable environment is based on the similarity of its geologic characteristics to the National Uranium Resource Evaluation (NURE) recognition criteria described in Mickle and Mathews (eds., 1978). The study was conducted by the Albuquerque, New Mexico, District Office of Bendix Field Engineering Corporation (BFEC) for the NURE program, managed by the Grand Junction Area Office of the U.S. Department of Energy (DOE).

ACKNOWLEDGMENTS

The authors acknowledge the personnel of the Gila Hot Springs Ranch for their hospitality and use of their riding and pack stock: in particular, we thank "Doc" and Ida Campbell and Tim and Becky Eichard. Thin-section analyses and mineral identifications were performed by Michael Eatough, Petrology Laboratory, BFEC.

SCOPE

Evaluation of the Clifton Quadrangle began January 1980 and terminated March 1, 1981. Approximately 2.5 man-years were expended by the authors and other BFEC personnel during literature search, field and laboratory study, evaluation of data, and preparation of the folio. An area of approximately 20,600 km^2 was evaluated during this study. However, access to the Fort Apache and the San Carlos Indian Reservations was restricted (Pl. 12), and permission to conduct studies was not obtained.

PROCEDURES

Literature research was done, and a study plan was formulated according to the information obtained from published sources.

In the field, uranium occurrences were examined (App. A). The geologic characteristics of the occurrences were noted, and rock samples were taken. Uranium-occurrence reports (App. C) were prepared on the basis of the field examinations, and geochemical data were added after sample analyses were completed (App. B).

The rock samples were analyzed for specific elements: chemical uranium (cU_3O_8) by fluorometric and colorimetric methods; equivalent uranium (eU), equivalent thorium (eTh), and potassium (%K) by gamma-ray spectrometry; trace elements by emission spectrometry; and major-element oxides by atomic absorption.

Thin sections of rock samples were analyzed to classify rock types and to identify alteration products, sulfides, clays, and uranium minerals. X-ray

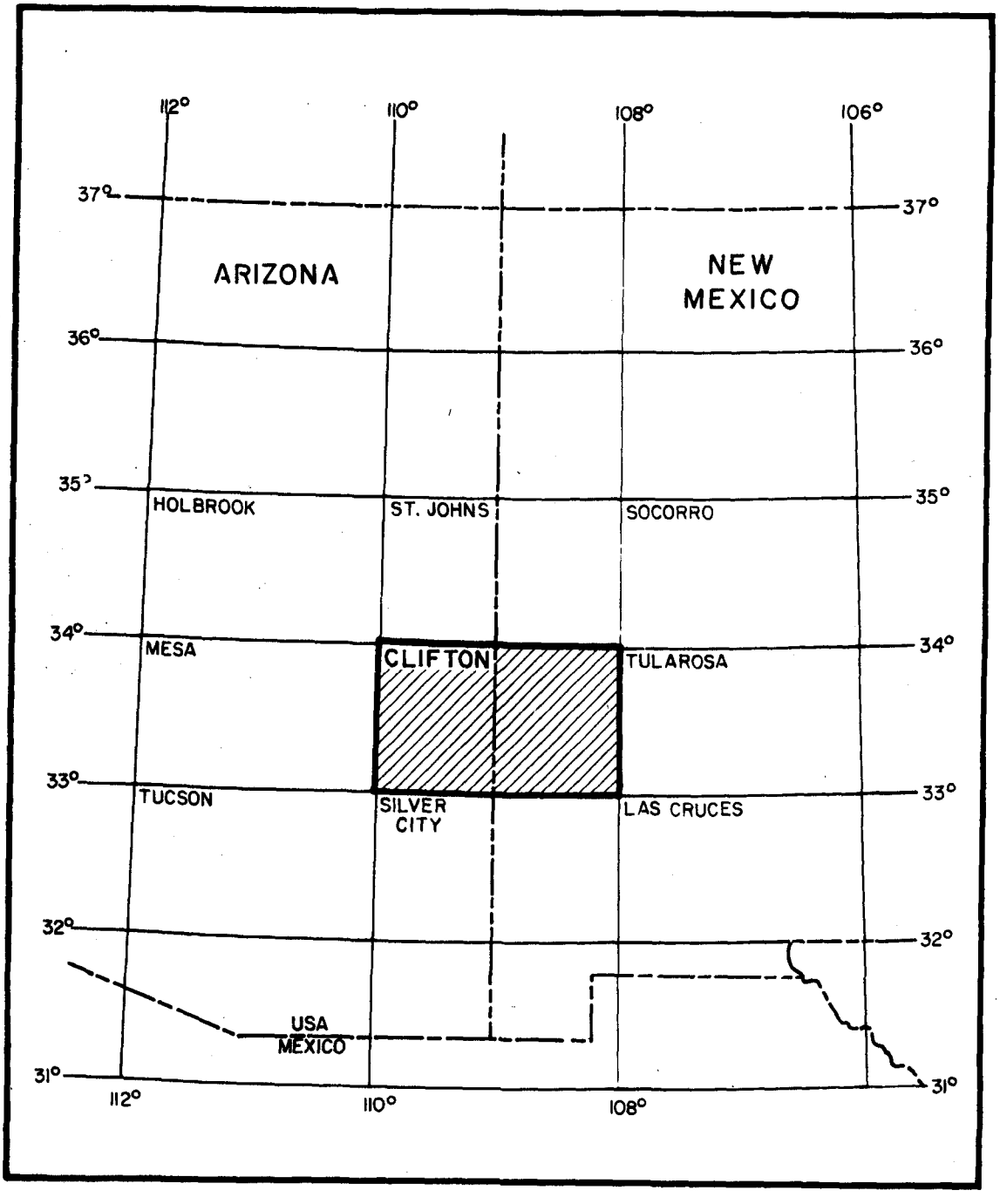

Figure 1. Location of Clifton Quadrangle.

diffraction, scanning-electron microscopy, and energy dispersal systems were used for minerals not identifiable in thin section. Petrographic reports are presented to Appendix D.

An aerial radiometric and magnetic survey (ARMS) was conducted by Texas Instruments, Inc. (1978), over the quadrangle at 4-mi (4.4-km) flight-line spacings. The radiometric data were interpreted by Texas Instruments, Inc., and BFEC to produce a radiometric anomaly map (Pl. 3) of the quadrangle. Radiometric traverses with hand-held scintillometers were conducted on foot and horseback in local areas to evaluate anomalies identified from ARMS data.

Hydrogeochemical and stream-sediment reconnaissance (HSSR) was conducted for the New Mexico part of the Clifton Quadrangle by the Los Alamos Scientific Laboratory. Data for the Arizona part of the quadrangle were not available for this study. The data for the New Mexico half of the quadrangle were interpreted by means of specific geochemical ratios to delineate areas of anomalously high uranium values (Pl. 4).

GEOLOGIC SETTING

The Clifton Quadrangle is between latitudes 33°00'00"N. and 34°00'00"N. and longitudes 108°00'00"W. and 110°00'00"W. The quadrangle is bisected at 109°04'30"W. by the Arizona-New Mexico state boundary. Parts of three physiographic provinces are present within the quadrangle: the Colorado Plateau in the northern part; the transition zone in the southwestern part; and the Basin and Range Province in the extreme southwestern part of the quadrangle. The most obvious topographic feature is the Mogollon Rim, which is present in the northern part of the quadrangle. The Mogollon Rim approximately defines the edge of the Mogollon Plateau (a subprovince of the Colorado Plateau), which is characterized by higher elevations as compared to the rest of the quadrangle (Fig. 2).

Rocks of Precambrian time are represented by a thick eugeosynclinal assemblage (Fig. 3a, 3b) of metamorphosed sandstone and shale, the Pinal Schist. The Pinal includes volcanic flows that range in composition from basaltic to rhyolitic. It has been intruded by plutons of granite to quartz monzonite compositions. The Pinal Schist was metamorphosed prior to emplacement of the plutons; the plutons do not show signs of metamorphism.

Paleozoic rocks unconformably overlie the Precambrian rocks. The Paleozoic was a time of marine deposition characterized by the accumulation of limestone, dolomite, sandstone, and shale (Fig. 3a, 3b). Sandstone units commonly have cross-stratification, interbedded conglomerate, and animal burrows and tracks. Limestone units are commonly massive and fossiliferous. They commonly contain lenses of chert and beds of dolomite. Shale occurs as interbeds within the sandstone. The shale is unfossiliferous and is commonly fissile. Paleozoic sediment-source areas were varied. There were repeated regressions and transgressions of the marine environment and, consequently, changing current directions. The rocks are laterally time transgressive.

Uplift, erosion, deposition, and intrusive activity occurred during Mesozoic time. Uplift during Triassic and Jurassic time caused erosion; sediments were deposited to the north and south of the Clifton Quadrangle, but

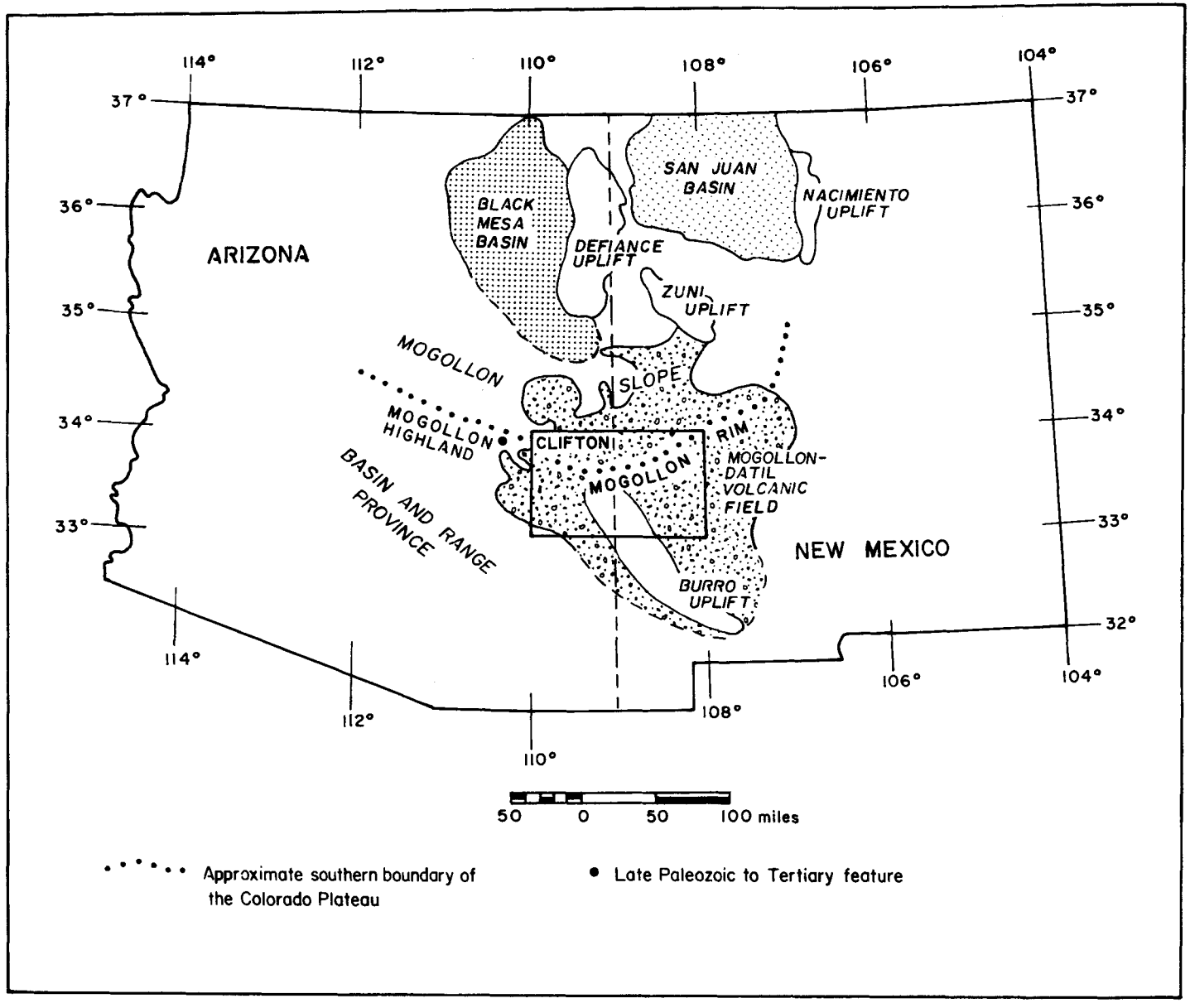

Figure 2. Generalized physiographic-tectonic location map of the Clifton Quadrangle.

there are no Triassic sedimentary rocks in the quadrangle. Intrusive rocks of Triassic age are found in the Clifton-Morenci area, in fault contact with older rocks. There are no rocks of Jurassic age in the quadrangle. Small Cretaceous stocks and sills unconformably overlie Paleozoic rocks near Clifton.

The Tertiary period was a time of extensive volcanism. The Mogollon-Datil volcanic field is a part of the mid-Tertiary volcanic field that extends from Oaxaca, Mexico, to southwestern Oregon, and the mid-Tertiary volcanic field is, in turn, a minor segment of the circum-Pacific belt. The Mogollon Plateau (Pl. 9), which lies within the Mogollon-Datil volcanic field, is interpreted as the physiographic expression of an underlying pluton (Elston and others, 1976).

Tertiary volcanic rocks were extruded from numerous calderas that formed during regional heating of the lithosphere. The composition of the volcanic rocks ranges from basaltic to rhyolitic. The volcanic rocks may be grouped into three chemical suites: a calc-alkalic suite, a high-silica alkali-rhyolite suite, and a basaltic-andesite suite. Radiometric ages of all the suites range from about 43 m.y. B.P. to the present.

Quaternary deposits are widespread. They include alluvium, basalt flows, interbedded sedimentary units, cinder cones, lacustrine deposits, and morainal material.

ENVIRONMENT FAVORABLE FOR URANIUM DEPOSITS

Area A, in the central part of the Clifton Quadrangle, lies along the ring-fracture system of the Bursum caldera (Pl. 1). It is favorable for magmatic-hydrothermal uranium deposits (Class 330, Mathews, 1978) because there is an inferred uranium source, there has been a possible passageway for fluids along the ring-fracture zone, and there is a suitable host rock.

The probable uranium sources are hydrothermal fluids from an inferred pluton and from the Whitewater Creek member of the Cooney tuff. The Whitewater Creek member has high silica and potassium contents, which indicate that the source magma was a late-stage differentiate.

The host rock is a fractured and sheared andesite dike. The dike contains such possible reductant sources as pyrite and clay gouge along fractures. The dike has been hydrothermally altered: it is silicified, and sericite, kaolinite, and chlorite have developed along shear zones.

Uranium minerals and anomalously high uranium contents of the rocks also indicate that a concentrating mechanism for uranium has operated. There are two uranium occurrences in the area. There are also base-metal sulfide deposits. Another favorable aspect is that the anomalously uraniferous rocks are represented by an aerial radiometric anomaly.

Those parts of the Cooney tuff that are covered by younger rocks are unevaluated because of the absence of subsurface data. It is probable that

other andesite dikes, presently covered, have intruded the Cooney tuff. The probability of such potentially favorable host rocks in the Cooney tuff enhances the favorability of Area A.

GENERAL GEOLOGY OF THE COONEY TUFF

The Cooney tuff, about 32 m.y. old (Ratte and others, 1978), is a compound cooling unit that was probably cauldron fill of the Mogollon caldera (Ratte and others, 1978). The Mogollon caldera predates development of the Bursum and Gila Cliff Dwellings calderas. The Cooney tuff is divided into the basal Whitewater Creek member, formerly the Whitewater Creek Rhyolite, and the upper Cooney quartz latite member, formerly the Cooney Quartz Latite (Ratte and others, 1978). The Cooney tuff is overlain by younger flows and is intruded by andesite sills and dikes along the ring-fracture zone of the Bursum caldera.

The Whitewater Creek member is a simple cooling unit that consists of densely welded ash-flow tuff. The base is not exposed, but thickness of exposed sections is 200 m. There is a 10-m-thick lithophysal zone near the bottom of the exposed section. The lithophysal zone indicates that the magma was gas charged and volatile rich during eruption.

The Cooney quartz latite member is about 400 to 500 m thick (Ratte and others, 1978). It is a compound cooling unit of ash-flow tuff that is partially welded in places and densely welded in other places; the pattern of welding is not yet understood. The tuffs are separated locally by sandstone and conglomerate. The tuffs contain 40 to 50 percent plagioclase, biotite, and opaque phenocrysts; the rest of the tuff consists of pumice fragments (Ratte and others, 1978).

The Cooney tuff was faulted during ring-fracture development of the Bursum caldera and is now exposed along Cooney Canyon and Whitewater Creek Canyons. It is intruded by numerous andesite sills and dikes.

During caldera development there were two major episodes of normal faulting in the Mogollon Plateau region. The first episode, more complex and extensive than the second, generated a set of faults that trend north-northeast. The second generated a set that trends west-northwest (Pl. 9). The first set has more displacement and is nearly vertical. Subsidiary fractures branch from the major faults.

Many of the main faults and their subsidiary fractures are occupied by veins, which were emplaced shortly after faulting. The veins result from volcanic activity and hydrothermal circulation during caldera development.

The later faults affected the earlier faults in a minor way. Even though the effect was minor, brecciated zones adequate for mineral deposition were produced. Clay gouge was also produced and probably aided mineralization by impeding fluid flow. These veins became the host for uranium.

Two types of veins are found in the Mogollon district. They differ in mineralogy and distribution. In the Cooney area, for example, veins contain

chalcopyrite, bornite, and chalcocite. They are from 2 to 5 m wide and from 100 to 200 m long. They are not restricted to faults and are widespread.

The second type of vein is restricted to faults. Most of the ore is in the northwest-trending faults. These veins are commonly from 1 to 4 m wide, but may be as much as 15 m wide. Metallic minerals in the second type of veins are pyrite, chalcopyrite, galena, bornite, argentite, stromeyerite, chalcocite, and tetrahedrite. Gangue minerals are predominantly quartz and calcite. Fluorite, colorless to light green, is concentrated near the center of the mining district. The presence of fluorite indicates that uranium could have migrated as uranyl fluoride, UF_6.

BABY MINE

The Baby Mine is in the Mogollon mining district, from which gold, silver, copper, and lead have been produced. In 1955, the first report of uranium from the district followed discovery of uranium in the Baby Mine. About 7 tons of low-grade, vanadium- and uranium-bearing ore was shipped to the Globe, Arizona, buying station.

The Baby Mine is in sec. 20, T. 10 S., R. 19 W. The deposit is an example of the second type of vein mentioned above. It is along a sheared, fractured, and slightly brecciated zone intruded by an andesite dike of the Last Chance andesite.

The andesite is a fine- to medium-grained, reddish-purple rock that intrudes the massive Whitewater Creek member of the Cooney tuff. The Whitewater Creek member is more resistant than the dike. The dike forms a negative topographic feature--a trenchlike depression that can be traced N. 70° W. for about 150 m along the south wall of Cooney Canyon. The dike is nearly vertical. It averages 7 m wide, but divides into several parallel dikes near its northwestern end, where it has an aggregate thickness of 15 m.

Most veins in the district are continuous, well-defined, sulfide-bearing, quartz-calcite veins. The vein at the Baby Mine differs in that there has been widespread dissemination of pyrite in the country rock and in the andesite dike. The disseminated pyrite indicates that the mineralization was magmatic-hydrothermal. Additional evidence for hydrothermal alteration is the bleached appearance of the andesite dike. Moreover, sericite, kaolinite, and chlorite have developed within the altered dike. Veinlets of dark quartz seal the rock.

The andesite dike also contains local concentrations of drusy quartz, calcite, pyrite, and colorless to light-green or dark-purple fluorite. These minerals occupy small fissures and fractures in hydrothermally altered portions of the dike. The purple fluorite, caused by metamictization, is associated with uranium-bearing zones. Minor amounts of copper, lead, and zinc minerals are found along the sheared surfaces of the dike.

Thin-section descriptions of samples MLQ 041, MLQ 564, and MLQ 527 are included in Appendix D. These describe the alteration of the andesite dike, the development of clay along fractures, and the decomposition of olivine to iddingsite. Sample MLQ 041 was X-rayed to determine the identity of an

unknown mineral. The mineral is amorphous; it may be a solidified hydrocarbon. Sample MLQ 564, from the Whitewater Creek member, is a silicified brecciated tuff that contains angular tuff fragments. Feldspar fragments are decomposing to clay. Only minimal welding is indicated by the condition of the shards.

Unidentified primary uranium minerals and vanadium minerals occur with purple fluorite and pyrite in brecciated zones (Collins, 1957). These veins vary in width from 3 to 18 cm and can be traced for 10 m along the southwestern border of the dike. A dark vanadium mica similar to roscoelite was identified (Collins, 1957). Widespread, small and spotty, high-grade concentrations of schroeckingerite form fracture coatings in the walls of the central part of the adit. A slightly radioactive coating of gypsum occurs in the eastern end of the adit.

Only surface samples could be taken during the present study because the adit is flooded. Previously reported sample analyses (Collins, 1957) are, therefore, presented in Table 1. Collins' samples contained an average of 9,196 ppm U_3O_8 and 7,280 ppm V_2O_5. Surface samples for the present study contained an average of 86 ppm U_3O_8 (Table 2). These high uranium contents suggest that a mechanism for uranium concentration operated in this area. Furthermore, the differences in uranium contents between the surface and subsurface rock samples indicate that the mechanism was more effective in the subsurface Eh-pH conditions.

The thorium-to-uranium ratios, except for that of MLQ 568, range from 1 to 8 (Table 2) and suggest that some of the surface samples have lost uranium. Surface samples are commonly coated with limonitic stains. The staining is a result of the oxidation of pyrite--this suggests that the uranium in the surface rocks may have been oxidized and mobilized. This would help to explain the low uranium content of the surface samples compared to high uranium contents of Collins' samples.

EVELYN CLAIMS

The Evelyn Claims are approximately 2 km south of the Baby Mine, along the ring-fracture system of the Bursum caldera, in sec. 5, T. 11 S., R. 19 W. An adit has been driven about 20 m in a northeast-trending, sheared and silicified zone in the Whitewater Creek member. Low radioactivity is found along a seam of clay gouge along a sheared surface. No uranium minerals were observed, but pyrite is ubiquitous throughout the area.

URANIUM GENESIS

Geologic events relating to uranium source, transport, and deposition of the Cooney tuff took place after the Mogollon caldera was filled with Cooney tuff. Stratigraphic and age relationships (App. E) indicate that development of the Bursum caldera and its ring-fracture zone occurred concurrently with the extrusion of large amounts of silicic, potassic, ash-flow-tuff units. The tuff units have a chemical nature indicating that the magma that generated them was a late-stage differentiate. This type of magma, theoretically, could contain large amounts of uranium. The uraniferous zones in the Cooney tuff,

TABLE 1. Chemical Analyses from the Baby Mine

Sample no.	U_3O_8 (ppm)	V_3O_8 (ppm)	Sample no.	U_3O_8 (ppm)	V_2O_5 (ppm)
F-46189*	1,700	10,700	F-32577*	1,400	7,200
F-46188*	5,800	12,700	F-32578*	200	4,500
F-32574*	87,600	18,200	F-46195*	1,180	4,700
F-32576	1,000	7,000	F-38638*	880	5,900
F046187*	1,200	8,300	F-46193*	8,710	4,000
F-38642*	5,400	10,200	F-38636*	10,100	2,500
F-46358*	2,900	8,000	F-38637*	31,800	5,200
F-46359	1,400	8,700	F-46191*	820	1,100
F-46360*	510	14,400	F-38639*	1,100	1,400
F-32575*	1,600	11,200			

*Values from Collins, 1957.

TABLE 2. Results of chemical uranium and equivalent potassium, uranium, and thorium

Sample no.	U O (ppm)	eK(pct)	eU(ppm)	eTh(ppm)
MLQ 528	7.0	5.0	9.0	11.0
MLQ 529	2.0	6.2	3.0	26.0
MLQ 564	1.0	---	---	---
MLQ 568	332.0	4.0	178.0	16.0

the reported primary and secondary uranium minerals, and anomalous uranium contents of the rocks support the idea of a uraniferous magma. A pluton of regional size has been inferred (Elston and others, 1976) to lie underneath the Mogollon Plateau. A pluton of this size should be an adequate uranium source.

The association of uranium and sulfide minerals with an andesite dike in the Whitewater Creek member of the Cooney tuff suggests that such dikes may have been particularly receptive to uranium deposition. Whether this was because of their particular physical properties or because of their chemical properties is not known.

Relationships between the ring-fracture zone, sulfide minerals, uranium minerals, and hydrothermal alteration indicate that the ring-fracture system acted as passageways for uraniferous hydrothermal solutions. The sulfide minerals and the argillic and sericitic alteration indicate that the solutions probably leached additional uranium from earlier tuff units and thereby supplemented the original uranium contents.

The probable mechanism of uranium transport in solution is indicated by the presence of fluorite. Uranium probably traveled as uranyl fluoride complex, UF_6. Uranium was deposited from the solution when the proper physical-chemical conditions were available.

Reducing conditions or trapping mechanisms for uranium may have been caused by changes in Eh-pH conditions, temperature-pressure changes, or the presence of pyrite. The association of uranium and pyrite supports the argument that, in this case, pyrite reduced uranium from the hydrothermal fluids. Uranium is found only where pyrite is found. Deposition of uranium was confined to brecciated, pyritic zones and cavities along the andesite dike.

Some secondary uranium and radioactive gypsum were probably deposited in recent time. Circulating ground water leached uranium from the uraniferous cones as well as from ash-flow-tuff units. These circulating waters deposited uranium along fractures and walls of abandoned adits.

SUMMARY

Area A encompasses the outcrop limit of the Cooney tuff. This has an area of approximately 45 km^2 and is at least 700 m thick. Its volume is about 32 km^3. An unknown number of hydrothermally altered zones are probably present in the subsurface. The area is in the Gila National Forest. Part of Area A is in the Gila Wilderness, which is a restricted area in the national forest.

ENVIRONMENTS UNFAVORABLE FOR URANIUM DEPOSITS

In the Clifton Quadrangle, unfavorable environments include plutonic (Classes 320 through 380, Mathews, 1978) for Precambrian rocks; marine black shale (Class 130, Jones, 1978) and limestone (Class 230, Jones, 1978) for

Paleozoic rocks; sandstone (Class 240, Austin and D'Andrea, 1978) for Paleozoic rocks and for Tertiary and Quaternary rocks; and volcanogenic (Classes 510 through 540, Pilcher, 1978) for Tertiary and Quaternary volcanic rocks.

PRECAMBRIAN IGNEOUS AND METAMORPHIC ROCKS

The Precambrian rocks of the Clifton Quadrangle are predominantly the Pinal Schist. The Pinal is a metamorphosed sequence of sedimentary rocks that were deposited in the eugeosynclinal environment. The geologic map (Pl. 7) indicates that granitic plutons intrude the Pinal; however, these intrusive bodies, although searched for, were not found by the authors.

The Pinal is a quartz-sericite schist cut by mafic dikes. The Pinal does not contain anomalous radioactivity, nor were samples of it (App. B-1, MLQ 038) anomalous in uranium content. A weak ARMS anomaly is shown on Plate 3, but a ground search did not reveal any anomalous radioactivity. Limonitic and hematitic staining, sulfides, and fluorite were not observed.

The Pinal is not a good uranium source rock because it does not have a silicic composition nor is it intruded by silicic plutons or pegmatite dikes. It is not a good host for uranium because it does not contain apparent reductants, evidence of uranium concentration, or evidence of alteration.

Therefore, it is unfavorable for contact-metasomatic (Class 340), pegmatitic (Class 320), magmatic-hydrothermal (Class 330), autometasomatic (Class 350), authigenic (Class 360), allogenic (Class 370), and anatectic (Class 380) uranium deposits.

MARINE BLACK SHALE

The Percha Shale and the Portal Formation are unfavorable for marine-black-shale uranium deposits (Class 130) because no reductants have been reported and no sources of uranium are known. Also, the shale facies of the Portal Formation were deposited in an open, nonrestricted marine environment, which was probably not conducive to the accumulation and preservation of organic matter.

Portal Formation

The Portal Formation is of early to late Late Devonian age. It is present in the southern portions of the quadrangle, where it unconformably overlies the Fusselman Dolomite of Silurian age (Fig. 3a). The Portal Formation is equivalent to the Morenci Shale of Lindgren (1905). The lower part of the Portal Formation is equivalent to the Martin Formation, and the upper part to the Percha Shale. The Portal Formation is a lithologic intermediate between these two other formations (Kottlowski, 1963).

At its type locality in the Chiricahua Mountains of southwestern Arizona, the Portal Formation has four informal members, which are, in ascending order, thin-bedded, alternating olive-gray calcareous shale and dark olive-gray,

shaly, aphanitic limestone; black, fissile shale; thin-bedded, olive-gray, alterating shale and limestone; and thin-bedded, alternating limestone and shale. The formation thins northward, and at Clifton the shaly limestone and black, fissile shale facies predominate. The formation was deposited in nearshore environments (Kottlowski, 1963). The amount of uranium present in a uraniferous marine black shale seems to be directly proportional to the amount of organic matter present (Jones, 1978). No organic matter or reductant has been reported in the Portal Formation. No source of uranium is known.

Percha Shale

The Percha Shale, of late Late Devonian age, is present in the southeastern part of the quadrangle. The Percha Shale has two members (Fig. 3b). The lower Ready Pay Member is composed of black, unfossiliferous shale and grades into the upper Box Member. The Box Member is composed of greenish, dark-gray shale with limestone nodules and argillaceous, fossiliferous limestone. The Percha Shale was deposited in a restricted, stagnant marine basin (Kottlowski, 1963). Uraniferous marine black shales are distinctly noncalcareous (Jones, 1978). An unfavorable feature of the Percha Shale is its calcareous nature. No organic matter or reductants, such as H_2S, are reported. No source of uranium is known.

LIMESTONE

The following units are unfavorable for limestone uranium deposits (Class 230): the El Paso Limestone; the Upman Dolomite, Aleman Dolomite, and Cutter Dolomite of the Montoya Dolomite; the Fusselman Dolomite; the Martin Formation; the Portal Formation; the Redwall Limestone; the Escabrosa Group; the Lake Valley Formation; the Kelly Limestone; the Madera Limestone; the Yeso Formation; the San Andres Limestone; the Horquilla Limestone; and the Fort Apache Member of the Supai Formation. These units are unfavorable because they lack a source of uranium, are not sapropelic, and were deposited in nonrestricted marine environments.

El Paso Limestone

The El Paso Limestone, of Late Cambrian to Early Ordovician age, is divided into two informal members (Fig. 3a, 3b). In Arizona, the lower member conformably overlies the Coronado Quartzite. The lower member is composed of locally glauconitic, sandy or silty dolomite interbedded with dolomitic sandstone. The lower member is equivalent to the Longfellow Limestone of Lindgren (1905). The upper member conformably overlies the lower member to the west in Arizona, and the Bliss Sandstone to the east in New Mexico. The gray, thin- to medium-bedded, silty limestone has been irregularly dolomitized. The El Paso Limestone was deposited in shallow subtidal and intertidal flat environments (Kottlowski, 1963). No source of uranium is known, and no reductants have been reported.

Montoya Dolomite

The Montoya Dolomite, of Middle Ordovician age, is divided into four members (Fig. 3a, 3b). These conformable members, in ascending order, are the Cable Canyon Sandstone, the Upman Dolomite, the Aleman Dolomite, and the Cutter Dolomite (Kottlowski, 1963). No source of uranium is known for the formation. No reductants have been reported.

Upman Dolomite. Conformably overlying the basal, Cable Canyon Sandstone, the Upman Dolomite was deposited in shallow marine waters. The gray to dark-gray, massive, medium-crystalline dolomite is a recrystallized crinoidal calcarenite. The member has lenses of light-gray, friable, saccharoidal, unfossiliferous sandstone that is locally porous. Some workers have combined the Cable Canyon Sandstone and Upman Dolomite into one member named the Second Value Dolomite (Kottlowski, 1963).

Aleman Dolomite. The marine Aleman Dolomite conformably overlies the Upman Dolomite in New Mexico, but because of postdepositional erosion, does not extend as far as Arizona (Fig. 3b). The member comprises nonporous, medium-gray, fine- to medium-crystalline dolomite and some calcidolomite. The dolomite has numerous chert flakes and silicified fossils (Kottlowski, 1963).

Cutter Dolomite. The upper Cutter Dolomite is a light-gray, aphanic to finely crystalline dolomite with scattered, small, brown chert nodules and stringers. The member is usually thin to medium bedded, but, in the area south of the quadrangle, it is massive. The Cutter Dolomite conformably overlies the Aleman Dolomite in New Mexico, but, because of postdepositional erosion, does not extend into Arizona. The Cutter is equivalent to the Valmont Dolomite of some workers. The member is marine and nonporous (Kottlowski, 1963).

Fusselman Dolomite

Because of postdepositional erosion, the Fusselman Dolomite (Fig. 3b) is present only in New Mexico, where it unconformably overlies the Cutter Dolomite. The Fusselman Dolomite is of Silurian age. The dolomite is grayish brown to dark gray, aphanic to coarsely crystalline, and massive. In the area south of the quadrangle, the chert nodules that characterize the formation in much of New Mexico are sparse. The formation was deposited in a marine environment (Kottlowski, 1963). No source of uranium is known, and no reductants are reported.

Martin Formation

The Martin Formation, of early Late Devonian age, is present in the western and southwestern portions of the Clifton Quadrangle. The Martin Formation is equivalent to the Morenci Limestone of Lindgren (1905) in the Clifton-Morenci district (Kottlowski, 1963). Teichert (1965) divided the

formation into the basal Beckers Butte Member and the upper Jerome Member (Fig. 3a). Both are of marine origin (Teichert, 1965).

The Beckers Butte Member unconformably overlies the Upman Dolomite, of late Middle Ordovician age. The Beckers Butte Member is a dense, brown, thick-bedded limestone and dolomite. It is conformably overlain by the Jerome Member. The Jerome Member has three informal units: a lower, fetid dolomite; a middle, aphanic dolomite; and an upper unit of interbedded sandstone, shale, dolomite, and limestone (Teichert, 1965). No source of uranium is known, and no reductants are reported.

Redwall Limestone

The Redwall Limestone (Fig. 3a), of Mississippian age, is present in the northwestern part of the quadrangle. The Redwall Limestone is composed of four members, of which the lower three are present within the study area (Fig. 3a). The basal Whitmore Wash Member unconformably overlies the Martin Formation. The member comprises thick-bedded to massive limestone and dolomite. Conformably overlying the Whitmore Wash Member, the Thunder Springs Member is composed of chert beds alternating with thin limestone and dolomite. The Mooney Falls Member consists of thick-bedded to massive limestone and dolomite and conformably overlies the Thunder Springs Member. These members represent two transgressions and a regression upon the Zuni-Defiance uplift. The formation was deposited in shallow- to moderately deep-marine environments. No sources of uranium or reductants are known.

Escabrosa Group

The Escabrosa Group (Fig. 3a), of Mississippian age, crops out in the southern part of the quadrangle. It is composed of two formations. The lowermost is the Keating Formation and the uppermost is the Hachita Formation (Kottlowski, 1963). No sources of uranium or reductants are known for the group.

Keating Formation. The Keating Formation is divided into two members. The lower, A Member, consists of crinoidal limestone, oolitic limestone, and dark-gray, coral-bearing, aphanic limestone. The upper, B Member, is composed of thin-bedded, highly cherty limestone. The sediments were deposited in deep-water marine environments (Kottlowski, 1963). The Keating Formation was deposited synchronously with the Whitman Wash and Thunder Springs Members of the Redwall Limestone (McKee and Gutshick, 1969).

Hachita Formation. The Hachita Formation conformably overlies the Keating Formation. The Hachita Formation is composed of gray, massive, crinoid-bearing limestone. It was deposited in deep-water marine environments (Kottlowski, 1963). The Hachita Formation is correlative with the Mooney Falls Member of the Redwall Limestone (McKee and Gutshick, 1969).

Lake Valley Formation

The lowest four of the six conformable members of the Mississippian Lake Valley Formation are present in the southeastern portion of the quadrangle, where they overlie the Percha Shale (Fig. 3b). The basal Andracito Member is composed of gray, thin-bedded, arenaceous limestone; dark-gray, thin-bedded cherty limestone; and dark-gray, silty, argillaceous limestone and silty shale. The overlying Alamogordo Member is a massive, dark-gray, cherty, microcrystalline limestone. The Nunn Member, the third member, has interbedded light-gray, limy shale; friable, fossiliferous, crinoidal limestone; and dark-gray, argillaceous, silty, nodular limestone facies. The youngest member present in the study area, the Tierra Blanca Member, is a massive, light-gray, crinoidal limestone that has abundant light-gray chert (Kottlowski, 1963). The formation was deposited in shallow-water, marine-shelf environments (Kottlowski, 1963) representing a regression of the waters from the shelf area (Armstrong, 1962). The Lake Valley Formation is equivalent to the Keating Formation of Arizona (Kottlowski, 1963). No sources for uranium or reductants are known for the Lake Valley Formation.

Kelly Limestone

The Kelly Limestone (Fig. 3b) extends from south of the quadrangle to northeast of the quadrangle. The Kelly Limestone conformably overlies the Lake Valley Formation. The limestone is gray, massive, crinoidal, and cherty (Kottlowski, 1963). It was deposited in a shallow-water marine-shelf environment (Armstrong, 1962). The Kelly Limestone is equivalent to the Hachita Formation of southeastern Arizona and to the upper two members of the Lake Valley Formation in southern New Mexico (Kottlowski, 1963). No source of uranium is known, and reductants have not been reported.

Madera Limestone

The Madera Limestone, of Pennsylvanian age, is the uppermost member of the Magdalena Group (Fig. 3b). The formation is present along the eastern part of the quadrangle. In the southeastern part of the quadrangle, the Madera Limestone is equivalent to the Syrena Formation. The Madera Limestone conformably overlies the Sandia Formation and consists of lower shale, limestone, and limestone-pebble conglomerate lithofacies, and an upper massive limestone (Kottlowski, 1963). The rocks were deposited in shallow-marine environments and shoal areas onlapping the east side of the Zuni-Defiance uplift (Armstrong, 1962). The granite rocks of the Zuni-Defiance uplift could have been a source of uranium. However, no reductants are known in the limestone.

Horquilla Limestone

The Horquilla Limestone (Fig. 3a), of Pennsylvanian age, is present in the southwestern portion of the quadrangle. The limestone unconformably overlies the Hachita Formation. The Horquilla Limestone has limestone and interbeds of shale and siltstone. The formation was deposited synchronously with the Naco Formation (Kottlowski, 1963). Sources for the clastics were the

Zuni-Defiance and Florida uplifts (Ross, 1973). These uplifts could have been a source of uranium. However, no reductants are known within the formation. One sample, MLQ 037, believed to be from this formation (App. B-1), yields values of 1 ppm cU_3O_8, 3 ppm equivalent uranium, and 19 ppm equivalent thorium.

Supai Formation

The Supai Formation (Fig. 3a) has four members, which, in ascending order, are the Amos Wash Member, the Big A Butte Member, the Fort Apache Limestone, and the Corduroy Member. The Amos Wash Member is discussed under the unevaluated Naco-Supai interval, and the Big A Butte and Corduroy Members are discussed under unfavorable sandstone environments. The formation crops out in the northeast corner of the quadrangle, where it conformably overlies the Naco Formation (Pl. 7).

The Fort Apache Limestone is the third member of the Supai Formation. The member consists of very fossiliferous limestone, dolomite, and evaporitic dolomite lithofacies. Although some terrigenous detritus is present, the member represents a minor marine transgression upon the advancing deltaic sediments of the Supai Formation (Winters, 1963). The deltaic sediments could have been a source of uranium, but no reductants are known.

San Andres Limestone

The San Andres Limestone (Fig. 3b), of Permian age, crops out in the northeastern part of the quadrangle (Pl. 7). It conformably overlies the Yeso Formation. The San Andres Limestone is yellowish- to dark-gray, thin- to massive-bedded, locally fossiliferous, magnesian limestone and dolomite, interbedded with calcareous siltstone and fine-grained sandstone (Foster, 1964). The formation is of nearshore-marine origin (McKee, 1938). The Zuni-Defiance uplift could have been a source for uranium. Traces of pyrite are reported (Foster, 1969); however, they are too finely disseminated to act as effective reductants for uranium.

SANDSTONE

The following units are unfavorable for sandstone (Class 240) uranium deposits: the Bliss Sandstone, the Coronado Quartzite, the Cable Canyon Sandstone Member of the Montoya Dolomite, the upper part of the Jerome Member of the Martin Formation, the Sandia Formation, the Abo Formation, the Yeso Formation, the Alpha Member and lower half of the Beta Member of the Naco Formation, the Big A Butte and Corduroy Members of the Supai Formation, the Coconino Sandstone, and the Gila Conglomerate. These units are unfavorable because they lack reductants in the form of carbonaceous trash or H_2S; most of them lack sources of uranium; and most were deposited in marine or marginal-marine environments, not the more favorable fluvial environments.

Bliss Sandstone

The Bliss Sandstone was deposited unconformably on the Precambrian basement in shallow waters by a marine transgression (Fig. 3b). The formation is of Middle Cambrian age. The sandstone is present in the New Mexico half of the Clifton Quadrangle and is laterally time transgressive with the Coronado Quartzite of Arizona. Basal beds are pebbly, siliceous hematitic sandstone with local conglomeratic elements and thin limestone and shale beds. The upper facies are limestone (Kottlowski, 1963).

Coronado Quartzite

The Coronado Quartzite of Arizona is a pale-red to olive-brown weathering, glauconitic sandstone (Fig. 3a). It varies from arkosic at the base to orthoquartzitic in the upper beds. Small- to medium-scale cross-beds, animal tracks, and burrows are common. The formation, middle to early Late Cambrian, represents beach and, possibly, dune sands deposited near the strand line of the Abrigo Sea. The formation unconformably overlies the Precambrian basement rocks (Kottlowski, 1963).

Cable Canyon Sandstone of the Montoya Dolomite

The Cable Canyon Sandstone is the lowest member of the late Middle Ordovician Montoya Dolomite (Fig. 3a, 3b). A description of the Montoya Dolomite is found under unfavorable limestone environments. The Cable Canyon Sandstone unconformably overlies the El Paso Limestone. The sandstone is light to medium gray, angular to well rounded, very coarse grained, and quartzose with minor feldspar. It is massively to thickly bedded and locally cross-laminated. The member is free of clays and is locally porous. Source of the clastics seems to have lain to the north to northwest. The Cable Canyon was deposited in shallow-marine waters (Kottlowski, 1963).

Jerome Member of the Martin Formation

A more complete description of the Martin Formation is given in unfavorable limestone environments. As is all of the lower Upper Devonian Martin Formation (Fig. 3a), the Jerome Member is of marine origin (Kottleski, 1963). It is divided into three informal units; the lower two are of dolomite and the uppermost is of interbedded shale, limestone, dolomite, and sandstone (Teichert, 1965). Source of the clastics may have been the Precambrian quartzite of the Zuni-Defiance uplift (Huddle and Dobrovolny, 1952). It is the uppermost unit that is unfavorable for sandstone uranium deposits because of its marine origin and lack of reductants.

Lower Naco Formation

The Naco Formation (Fig. 3a), of Pennsylvanian age, is present in the northwestern part of the quadrangle. The formation has three members which, in ascending order, are the Alpha Member, the Beta Member, and the Gamma Member (Brew, 1965). The upper part of the Beta Member and the Gamma Member are discussed under unevaluated environments.

The basal Alpha Member was deposited on karst topography developed in the Redwall Limestone (Huddle and Dobrovolny, 1952). This lower member is composed of a basal chert breccia in a dark-reddish-brown mudstone and siltstone matrix overlain by stratified reddish-brown mudstone, siltstone, and fine-grained sandstone and minor limestone (Brew, 1965). The lower part of the member is an ancient soil (Huddle and Dobrovolny, 1952), whereas the upper part represents fluctuating marine and fresh-water environments (Brew, 1965).

The middle Beta Member was deposited in environments varying from marginal-marine to continental (Brew, 1965). The member is composed of a repeated sequence of limestone and noncalcareous units of shale, mudstone, and shaly siltstone (Brew, 1965). No carbonaceous trash is reported in the lower half of this member (Peirce and others, 1976). Sources of the clastics were the Kaibab uplift and the prograding delta of the Supai Formation (Brew, 1965). Although a possible source of uranium for the lower Naco Formation exists in the granitic rock of the Kaibab uplift, the predominantly marine environments and lack of reductants make it unfavorable.

Big A Butte and Corduroy Members of the Supai Formation

The Supai Formation (Fig. 3a) is present in the northwestern part of the quadrangle. The Pennsylvanian-Permian formation is an advancing, continental deltaic deposit with minor marine-transgressive beds (Winters, 1963). The formation is divided into four members--the basal Amos Wash Member, the Fort Apache Limestone, and the uppermost Corduroy Member. The Amos Wash Member is discussed under unevaluated environments, and the Fort Apache Limestone is discussed under unfavorable limestone environments.

The Big A Butte and Corduroy Members are of Permian age. They both are composed of reddish-brown sandstone, mudstone, and siltstone with thin interbeds of limestone and calcareous claystone, and stringers of gypsum (Winters, 1962). The members were deposited in mixed continental and marginal-marine environments (Winters, 1965; Ross, 1978). Sources for the detritus were probably the Zuni-Defiance and Uncompahgre-San Luis uplifts (Winters, 1963). The rocks of the uplifts could have been a source of uranium. However, no carbonaceous trash is reported in these members. At the time of deposition, an oxidizing environment was present, as is evidenced by the red color of the sediments. Any carbonaceous trash present at the time of deposition was probably oxidized.

Sandia Formation

The Sandia Formation is the lowest formation in the Magdalena Group (Fig. 3b). This formation, of Pennsylvanian age, unconformably overlies the Kelly Limestone in the northeastern portion of the quadrangle and the Lake Valley Formation in the southeastern part. The Sandia Formation is contemporaneous with the Horquilla Limestone and may be laterally continuous with it. The Sandia Formation consists of shaly limestone, shale, and limestone. The lower sandstone units are arkosic. The formation was deposited in shallow-marine environments and shoal areas onlapping the eastern side of the Zuni-Defiance uplift (Kottlowski, 1963). The granitic rocks of the Zuni-Defiance uplift were a possible source of uranium, but no reductants are known in the formation.

Abo Formation

The Abo Formation (Fig. 3b) is of Pennsylvanian-Permian age. It unconformably overlies Precambrian rocks of the Zuni-Defiance uplift to the north of the quadrangle, and probably conformably overlies the Madera Limestone, of Pennsylvanian age, within the northeastern corner of the quadrangle (Pl. 7). It is composed of reddish-brown, poorly sorted, quartzose or arkosic sandstone, and gray, red, and brown dolomite-cemented shale and silstone (Foster, 1964). Foster (1964) reported a basal, arkosic conglomerate, but did not give an areal extent. The rocks are a continental to marginal-marine deposit (Foster, 1964). No reductants have been reported in the formation.

Yeso Formation

The Yeso Formation (Fig. 3b), of Permian age, conformably overlies the Abo Formation (Pl. 7). The Yeso Formation is composed of olive, light-red, and gray sandstone interbedded with limestone and gypsum. It is a marginal-marine deposit (Foster, 1964). Winters (1963) suggested that, on the basis of similar lithologies, age, some common fauna, and similar depositional environments, the upper Supai Formation and the Abo and Yeso Formations may be equivalent. No reductants are known in the Yeso Formation.

Coconino Sandstone

The Coconino Sandstone (Fig. 3a), an eolian sandstone of Permian age, crops out in the northwest corner of the quadrangle (Pl. 7). The Coconino conformably overlies the Supai Formation. The sandstone is white to pale yellow, very fine to coarse grained, well sorted, quartzose, and cemented with either calcium carbonate or silica (Foster, 1964; Winters, 1963). Large-scale, well-developed, trough cross-bedding is distinctive (Winters, 1963). Secondary pyrite is found in trace amounts (Foster, 1964), and shows of gas and oil are reported (Peirce and others, 1970). However, they are too finely disseminated to have been effective reductants for uranium. No source of uranium has been reported.

CENOZOIC VOLCANIC ROCKS

The Tertiary-Quaternary rocks of the Clifton Quadrangle are predominantly volcanic. They range in composition from basaltic to rhyolitic and are widespread throughout the quadrangle. Although many of the units contain high weight-percentages of silica and are formed by resurgence of large cauldrons, they are unfavorable for volcanogenic uranium deposits (Classes 510, 520, 530, and 540, Pilcher, 1978) because of the absence of reductants and the lack of evidence indicating that concentrating mechanisms have been operative.

There are numerous formations that can be grouped into suites on the basis of rock chemistry, the suites representing genetic units. For the sake of simplification, the unfavorability of the volcanic units will be discussed by chemical suites, except for those units in the Datil Group.

Datil Group

The Datil Group includes volcanic rocks that range in composition from basaltic to rhyolitic. It contains some interbedded sedimentary units. The Datil overlies the Baca Formation (Fig. 3c) in the northern part of the quadrangle, south of the San Agustin Plains. The rocks of the Datil are commonly faulted and fractured and contain secondary chalcedony that has been precipitated from ground water. However, these chalcedony veins are not uraniferous.

Silicic ash-flow tuffs are widespread and show weak ARMS anomalies that suggest slight uranium concentration, but ground searches failed to indicate areas of uranium concentration. Although these volcanic rocks could have been a good uranium source, and the secondary chalcedony indicates ground-water movement, no reductants are present to trap and concentrate uranium. The mafic rocks of the Datil are also unfavorable for uranium deposition because they do not contain reductants.

Calc-Alkalic Suite

The calc-alkalic suite includes units of the Mogollon Plateau (Elston and others, 1976) and other areas. It is composed of andesitic to rhyolitic rocks. The sources were probably stratovolcanoes developed from shallow asymmetrical calderas (Elston and others, 1976). The silicic ash-flow-tuff units in the suite deserve consideration as possible uranium host rocks.

The silicic ash-flow tuffs are flow banded, indicating that the ash-flow tuffs were hot at the time of eruption. Lithophysae indicate that the ash flows had significant volatile contents; this is important in uranium transport. The lithophysae are filled with secondary silica, which indicates that mineral-rich fluids permeated parts of the tuff units. Celadonite, a hydrous silicate of iron, magnesium, and potassium, is found as vein fillings. Fluorine values are high in samples MLQ 554 and MLQ 032 when compared to average crustal values (Pilcher, 1978).

The silicic tuffs have unfavorable features that outweigh the favorable features mentioned above, however. The average equivalent-uranium content is only 3 ppm, a content lower than normal for silicic ash-flow tuffs, indicating that these are not uraniferous units. The thorium-to-uranium ratio is about 6, which suggests that significant leaching has not occurred either (Tables 3 and 4). These data argue against postdepositional uranium leaching, uranium transport, and secondary uranium concentration.

An additional unfavorable aspect of the suite is the absence of a correlation between uranium and total alkalis in samples representative of the calc-alkalic suite. A weak correlation was observed between uranium and fluorine. The results indicate that the high alkali content or fluorine content of the unit does not mean that there will be a corresponding high content of uranium.

Aerial radiometric anomalies (Pl. 3) are present along the ring-fracture zone of the Bursum and Gila Cliff Dwellings calderas. These, however, probably reflect subtle differences in lithologies; no anomalously high

TABLE 3. Selected analyses of the calc-alkalic suite

Formation	Sample no.	cU 0 (ppm)	eK (%)	eU (ppm)	eTh (ppm)	Th/U
Railroad Canyon Tuff	MLQ 501	7.0	4.1	6.0	37.0	6.0
Tuff of Davis	MLQ 044	---	4.7	2.0	21.0	11.0
	MLQ 062	2.0	4.0	6.0	27.0	5.0
Tuff of Shelly Peak	MLQ 048	3.0	3.3	4.0	17.0	5.0
	MLQ 544	---	4.4	6.0	28.0	5.0
	MLQ 574	---	4.2	2.0	15.0	8.0
	MLQ 575	---	4.9	3.0	19.0	6.0
	MLQ 061	10.0	4.0	4.0	23.0	6.0
Alum Mountain (includes Murtocks Hole and Gila Flat)	MLQ 029	2.0	1.2	1.0	1.0	1.0
	MLQ 030	3.0	3.3	1.0	0.0	---
	MLQ 031	3.0	2.7	2.0	0.0	---
	MLQ 032	6.0	4.2	4.0	40.0	10.0
	MLQ 545	3.0	3.4	8.0	35.0	4.0
	MLQ 546	1.0	2.6	0.0	6.0	---
	MLQ 547	3.0	1.4	1.0	5.0	---
	MLQ 554	10.0	---	---	---	---
	MLQ 555	3.0	3.9	8.0	37.0	5.0
	MLQ 556	19.0	1.6	2.0	5.0	3.0
	MLQ 577	3.0	1.7	2.0	9.0	5.0
	MLQ 578	1.0	1.5	2.0	9.0	5.0
	MLQ 570	---	3.5	3.0	13.0	4.0
	MLQ 571	---	3.3	3.0	11.0	4.0
	MLQ 579	---	2.5	3.0	16.0	5.0
	MLQ 580	---	4.9	2.0	22.0	11.0
	MLQ 581	---	4.2	4.0	21.0	5.0
	MLQ 582	---	4.8	4.0	20.0	5.0

TABLE 4. Major oxide chemical data for the calc-alkalic suite

Sample No.	Al_2O_3	K_2O	Na_2O	CaO	FeO	Fe_2O_3	MgO	SiO_2	TiO_2	MnO	F(ppm)	S	Agpaitic Coefficient
MLQ 546	18.33	2.85	3.47	4.46	0.16	5.11	3.37	61.18	1.09	0.08	-	<0.01	0.48
MLQ 547	16.76	1.42	3.87	4.61	<0.10	11.83	5.75	49.60	1.10	0.17	-	<0.01	0.47
MLQ 554	16.18	4.71	4.57	1.12	0.16	1.37	0.61	73.70	0.47	0.07	891	0.01	0.78
MLQ 555	13.33	4.07	3.87	5.80	0.25	0.19	0.19	74.50	0.17	0.06	551	0.01	0.81
MLQ 556	17.87	1.55	3.33	8.40	1.49	7.31	6.71	56.09	1.12	0.18	632	0.01	0.40
MLQ 501	11.43	4.87	3.59	0.25	0.04	1.07	0.18	77.63	0.16	0.09	-	-	0.20
MLQ 029	17.17	0.93	3.05	8.40	1.26	8.66	5.02	56.73	1.49	0.13	-	<0.01	0.34
MLQ 030	17.03	3.14	3.61	5.40	0.21	7.97	2.68	60.48	1.25	0.10	401	0.02	0.54
MLQ 031	12.76	2.29	1.25	3.46	<0.10	3.79	1.77	60.39	0.72	0.06	<200	<0.01	0.36
MLQ 032	16.88	3.77	3.52	3.74	0.58	3.03	2.68	69.49	0.80	0.08	827	<0.01	0.58

radioactivity was observed during ground checking of the aerial anomalies. HSSR results (Pl. 4) suggest a possible uranium enrichment along the ring-fracture system of the Gila Cliff Dwellings caldera (see interpretation of hydrogeochemical and stream-sediment reconnaissance, this report).

In the absence of vanadates and phosphates which can retain uranium in the oxidized state, reductants, such as sulfides, or reducing mechanisms are critical for uranium deposition. Except at the Baby Mine and at Alum Mountain, sulfides were not found in the calc-alkalic suite. Evidence for such possible reducing mechanisms as Eh-pH or temperature-pressure changes was not observed. As pointed out in the discussion of the Baby Mine, uranium is observed only where sulfides are present.

The calc-alkalic suite does have favorable characteristics, such as high silica values, one favorable agpaitic coefficient, quartz latitic lithologies, and associated ARMS and HSSR anomalies. Also, silicic ash-flow tuffs in the sequence theoretically could have been good uranium source rocks. This suite does not have anomalous concentrations of uranium, however. Also, the mafic phase of the suite is a poor source of uranium. No sulfides or other possible reductants are known to be present. This suite is unfavorable for deposition of uranium in Classes 510, 520, 530, and 540.

High-Silica Alkali-Rhyolite Suite

This suite consists of quartz-sanidine-plagioclase-biotite ash-flow tuff, flowed-banded rhyolite, and ring-fracture and moat deposits. The rocks (App. D) range from crystal poor to crystal rich. Most of the rocks are rhyolitic; some are dacitic and andesitic.

Some of the rocks in this suite contain lithophysal cavities filled with chalcedony. Other samples have pumice fragments, glass, ash, and plagioclase crystals, which indicate a gas-charged magma. Minor devitrification occurred after eruption. Rhyolitic domes are found throughout the volcanic sequence.

Airborne radiometric anomalies are found throughout the high-silica alkali-rhyolite suite, but ground searches failed to locate the sources of radioactivity. HSSR data did not identify areas of anomalously high uranium. However, a weak anomaly that may indicate uranium concentration at the Tertiary-Paleozoic contact is discussed in the unevaluated section.

Chemical data and gamma-ray spectrometric data for the suite (Table 5) indicate that equivalent uranium averaged 7 ppm, potassium averaged 4.3 ppm, equivalent thorium averaged 23 ppm, and the thorium-to-uranium ratio was 5. Although sample MLQ 065 contains 51 ppm equivalent uranium and has a thorium-to-uranium ratio of less than 1, surrounding rocks contain no anomalous uranium. Thorium contents are not anomalous, and the thorium-to-uranium values are within the normal range of crustal rocks. This indicates that uranium leaching has probably not occurred.

The rocks are high in silica and total alkalis and low in calcium, iron, and magnesium (Table 6), as is typical of rhyolitic rocks. The agpaitic coefficients are commonly high, which indicates the eruption of a late-stage magmatic differentiate.

TABLE 5. Selected values of high-silica-alkali-rhyolite suite

Formation	Sample no.	cU_3O_8 (ppm)	eK (%)	eU (ppm)	eTh (ppm)	Th/U
Apache Springs Quartz latite	MLQ 512	2.0	4.9	3.0	16.0	5.0
	MLQ 533	7.0	3.8	5.0	24.0	5.0
	MLQ 583	---	4.7	4.0	19.0	5.0
	MLQ 584	---	5.7	5.0	22.0	5.0
	MLQ 585	---	4.4	3.0	17.0	5.0
	MLQ 586	---	4.7	3.0	16.0	5.0
	MLQ 587	---	5.9	3.0	14.0	5.0
	MLQ 589	---	3.9	4.0	17.0	5.0
	MLQ 592	---	4.0	5.0	24.0	5.0
	MLQ 594	---	4.0	4.0	29.0	4.0
Bloodgood Canyon Rhyolite Tuff	MLQ 060	4.0	3.8	17.0	28.0	2.0
	MLQ 536	3.0	4.1	4.0	33.0	8.0
	MLQ 537	3.0	4.1	7.0	22.0	3.0
	MLQ 538	5.0	4.6	7.0	31.0	4.0
	MLQ 539	<1.0	4.3	6.0	34.0	6.0
	MLQ 542	6.0	4.6	5.0	35.0	6.0
	MLQ 548	<1.0	4.0	7.0	38.0	4.0
	MLQ 551	1.0	4.3	6.0	32.0	5.0
Tuff of Fall Canyon	MLQ 049	4.0	---	---	-----	---
	MLQ 572	---	2.9	2.0	11.0	6.0
	MLQ 573	---	3.9	2.0	16.0	8.0
	MLQ 576	---	2.3	8.0	27.0	3.0
Sacaton Mountain Quartz Latite	MLQ 593	---	3.7	4.0	17.0	4.0
Fanney Rhyolite	MLQ 511	3.0	4.8	3.0	5.0	2.0
	MLQ 514	2.0	7.5	4.0	27.0	7.0
	MLQ 535	24.0	3.0	13.0	21.0	2.0
Jerky Mountain	MLQ 064	10.0	4.1	7.0	32.0	4.0
	MLQ 065	74.0	4.0	51.0	31.0	0.6
	MLQ 552	<1.0	4.4	5.0	31.0	6.0

TABLE 5. Selected values of high-silica-alkali-rhyolite suite (cont)

Formation	Sample no.	cU_3O_8 (ppm)	eK (%)	eU (ppm)	eTh (ppm)	Th/U
Jerky Mountain	MLQ 553	4.0	4.3	4.0	22.0	5.0
	MLQ 559	4.0	4.5	4.0	3.0	1.0
Tuff of Diablo Mountain	MLQ 033	6.0	4.8	5.0	4.0	1.0
	MLQ 034	9.0	3.8	6.0	28.0	5.0
	MLQ 035	5.0	2.7	4.0	20.0	5.0
	MLQ 549	5.0	4.3	7.0	39.0	6.0
	MLQ 550	<1.0	4.6	9.0	30.0	3.0
Willow Creek	MLQ 534	5.0	3.9	5.0	21.0	4.0

TABLE 6. Major oxide chemical data for the high-silica alkali-rhyolite suite

Sample no.	Al_2O_3	K_2O	Na_2O	CaO	FeO	Fe_2O_3	M_2O	SiO_2	TiO_2	MnO	F	S	Agpaitic Coefficient
MLQ 512	12.45	6.11	4.43	0.96	0.20	0.20	0.72	67.79	0.74	0.06	---	----	0.23
MLQ 512	14.31	5.66	2.64	0.57	0.24	0.79	1.55	76.99	0.27	0.05	234	<0.01	0.73
MLQ 536	13.27	5.03	3.47	0.41	0.26	0.64	0.32	78.08	0.19	0.04	256	<0.01	0.8
MLQ 538	13.85	5.34	3.87	0.88	<0.10	0.60	0.39	77.28	0.19	0.05	1302	<0.01	0.87
MLQ 539	13.62	5.03	3.26	0.37	<0.10	0.88	0.28	76.12	0.17	0.06	266	0.09	0.79
MLQ 542	15.14	4.71	3.19	0.24	0.18	0.89	0.24	75.53	0.22	0.04	767	<0.01	0.68
MLQ 548	22.72	4.07	3.87	0.11	<0.10	0.62	0.12	79.74	0.14	0.04	---	<0.01	0.47
MLQ 551	13.12	4.07	3.87	0.33	0.16	0.71	0.16	80.65	0.25	0.06	585	<0.01	0.82
MLQ 552	17.49	3.46	4.92	2.66	0.30	1.65	0.62	71.45	0.42	0.08	917	<0.01	0.67
MLQ 553	13.32	4.02	3.87	0.23	0.10	0.76	0.22	78.41	0.21	0.05	434	0.01	0.80
MLQ 559	16.41	5.34	3.87	0.30	0.21	0.65	0.13	46.97	0.21	0.04	250	0.01	0.74
MLQ 033	13.62	4.40	3.17	0.24	<0.10	0.92	0.19	64.71	0.25	0.05	271	<0.01	0.73
MLQ 034	11.23	3.14	0.76	2.52	<0.10	0.92	0.69	50.46	0.22	0.06	<200	<0.01	0.41
MLQ 035	16.71	2.85	3.87	7.27	0.90	4.66	3.59	60.03	0.78	0.13	528	<0.01	0.57
MLQ 549	15.09	4.40	0.64	1.02	<0.10	0.38	0.15	71.18	0.11	0.13	---	<0.01	0.38
MLQ 550	13.76	4.40	3.87	0.31	0.20	1.01	0.22	77.87	0.25	0.06	755	<0.01	0.81

Fluorine content of the high-silica alkali-rhyolite is high when compared to crustal averages of the same rock type. Fluorine and uranium commonly travel together as a uranyl-fluoride complex in magmatic-hydrothermal systems. However, the correlation coefficient between uranium and fluorine for this suite indicates no correlation between the variables. This suggests that although fluorine is a common constituent of the suite, uranium is not necessarily associated with fluorine in the suite. Furthermore, if uranium is associated with fluorine, the uranium content does not have to be elevated above crustal values to the same degree as fluorine.

The high-silica alkali-rhyolite suite is a good source of uranium. The Na_2O, K_2O, agpaitic coefficient, and mineralogy indicate that the suite is a late-stage differentiate. Fluorite and anomalous fluorine contents in the rocks also indicate this suite is a good source because of the association between fluorine and uranium.

The suite is, however, an unfavorable host for uranium. The uranium and thorium contents are low and the thorium-to-uranium ratio does not suggest significant leaching of uranium. Furthermore, the absence of a reducing or concentrating mechanism means that uranium will not be deposited. No evidence was found to indicate that such reducing mechanisms as Eh-pH changes or temperature changes were operative. Absence of sulfide minerals in this unit is important in the Clifton Quadrangle because uranium concentrations are found only where sulfide minerals are found. Also, the pyroclastic origin of this suite tends to disseminate uranium over large areas rather than concentrate uranium. Furthermore, there is no indication of hydrothermal alteration that, in turn, could suggest that mineralization took place.

In summary, the high-silica alkali-rhyolite is unfavorable for uranium deposits of Classes 510, 520, 530, and 540 because no reducing or trapping mechanisms were observed. Aerial anomalies were not located during ground searches, the uranium and thorium contents are not anomalously high, and formation of the silicic ash-flow tuffs tends to disseminate rather than concentrate uranium.

Basaltic Andesite Suite

The basaltic andesite suite is unfavorable for uranium deposits of volcanogenic origin (Classes 510, 520, 530, 540) because it is a poor source of uranium and no reductants or evidence for trapping mechanisms were observed. Moreover, it does not contain ARMS anomalies, and it does not have anomalously high uranium content.

Cenozoic Basalt

Tertiary-Quaternary basalts include those of the White Mountain volcanic field and unnamed basalt flows between Springerville and Clifton (Pl. 7). The basalt flows of the White Mountain volcanic field are alkali-calcic (Merrill, 1974). They formed from a deep-seated, primitive magma. The volcanics formed in a tensional regime created by the intersection of the Jemez Lineament and the Capitan Lineament (Chapin and others, 1978).

The mafic nature of these rocks indicates that they are a poor source of uranium. Radiometric traverses failed to locate any anomalously high radioactivity. The ARMS and HSSR surveys also did not detect areas of anomalously high radioactivity. Reductants were not observed, nor were structures that might have acted as traps or provided concentrating mechanisms.

UNEVALUATED ENVIRONMENTS

Unevaluated areas include those where access was restricted and those where conflicting or insufficient data did not permit an evaluation. Some private lands and the White Mountain Apache and San Carlos Indian Reservations were not evaluated because of access restrictions. Areas where conflicting or insufficient data prevented evaluation include the Red Mountain caldera, Alum Mountain, and the regional unconformity between the Paleozoic units and Tertiary volcanic rocks.

RED MOUNTAIN CALDERA

The Red Mountain caldera is in the Blue Range Wilderness in the west-central part of the quadrangle, between Alpine and Clifton, Arizona. Its geology has been studied by Ratte and others (1969). A generalized stratigraphic column is shown in Figure 4. The area was not studied in the field because its rugged topography required excessive travel time. The time constraints precluded evaluation of the area within the time frame of the project.

Red Mountain is a 2-km-wide by 4-km-long subcircular caldera. The basal part of the caldera is a pyroxene-hornblende andesite (Ratte and others, 1969). The caldera is filled with a rhyolitic ash-flow tuff, approximately 230 m thick, that is overlain and intruded by a rhyolite. The ash-flow tuff is composed of two cooling units--an upper unit and a lower unit. Overlying the rhyolite of Red Mountain is a basaltic-andesite unit that contains an interbedded peralkaline ash-flow tuff. Local unconformities are numerous in the volcanic sequence.

Three major trends of faults are observed in the Blue Range Wilderness--northeast, northwest, and west. The faults are steep, normal faults with displacements ranging from 3 m to more than 300 m. Displacement of the pre-Gila Conglomerate rocks is commonly greater than displacement of the Gila Conglomerate, indicating that much of the movement occurred prior to disposition of the Gila. The Blue Fault zone is the major fault zone and consists of several northeast-trending belts that define a 15- to 45-km-wide graben that cuts a northwest regional structural trend.

The area has favorable attributes, such as rhyolitic and peralkaline rocks that could have been sources of uranium. The rocks are possible uranium host rocks, as well. Major-oxide data (Ratte and others, 1969) show the ash-flow tuff and rhyolite have greater than 70 weight-percent silica and have agpaitic coefficients greater than unity. An ARMS anomaly (Pl. 3) is present over the area of Red Mountain. Fluorite has been reported in adjacent areas.

SERIES	FORMATION	RADIOMETRIC AGE (METHOD)	LITHOLOGY	DESCRIPTION
OLIGOCENE-MIOCENE	Gila Conglomerate		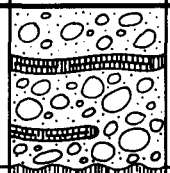	Buff to gray, boulder conglomerate, locally derived, interlayered with basaltic flows.
	Basaltic andesite	23.3 ±0.7 m.y. (K-Ar: whole rock)	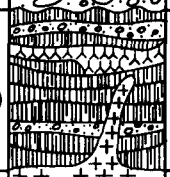	Black to dark-gray, holocrystalline, vesicular to amygdaloidal basaltic andesite flows intertonguing locally with thin gravel beds and a peralkaline, rhyolitic ash-flow tuff
	Quartz latite and rhyolite complex	23.4 ±0.7 m.y. (K-Ar: biotite)	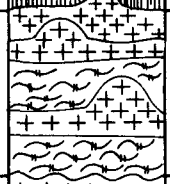	Extrusive-intrusive dome complex; dikes of complex intrude lower lava flows of basaltic andesite[1]
	Rhyolite tuff	24.9 ±0.7 m.y. (K-Ar: sanidine)	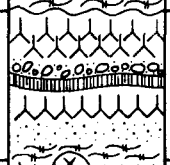	Welded rhyolite ash-flow tuff sheet interlayered with conglomerate, sandstone, andesitic lava flows, and other rhyolite and quartz latite ash-flow sheets[2]
	Rhyolite of Red Mountain		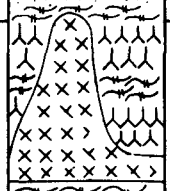	Welded rhyolite ash-flow tuffs, lava flows, and intrusive rhyolite[1]
EOCENE-OLIGOCENE	Pyroxene-hornblende andesite	37.4 ±3.9 m.y. (K-Ar: horn blende)		Lava flows, flow breccias, and pyroclastic breccias of pyroxene-hornblende andesite, cut by dikes of the same composition[1]
	Epiclastic volcanics		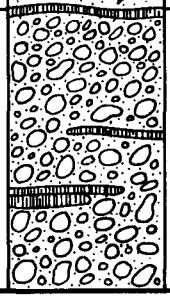	Includes some andesitic to dacitic lava flows and epiclastic conglomerate containing clasts of fossiliferous limestone and gneissic granite[2]

[1]Southern half of primitive area only.

[2]Northern half of primitive area only.

Figure 4. Stratigraphic column of Red Mountain, Arizona.

Previous work by Ratte and others (1969) did not include uranium analyses, and samples were not collected during the present study. Thus, an estimate as to grade of potential uranium deposits cannot be made.

ALUM MOUNTAIN AREA

The Alum Mountain area is in the southeastern part of the quadrangle. The stratigraphic sequence consists of andesite, sandstone, latite, and basaltic-andesite (Pl. 10). An adit, about 2 m wide, 2 m high, and 50 m long, has been excavated near Alum Mountain.

The area was hydrothermally altered by circulating magmatic fluids during volcanism, and rocks at the adit of the Alum Mine have been bleached white. The color of the rocks changes from white to orange to red away from the adit. The country rock is less intensely altered, but shows limonitic and hematitic iron stains.

Alum was deposited along a fault and fracture system. The country rock is also brecciated. The alum was precipitated from hydrothermal fluids derived from local vents in the area. Sulfides were not observed, but black manganese staining occurs in some places.

The area has low uranium contents but is slightly enriched in molybdenum and vanadium (Table 7). There is a slight correlation between vanadium and molybdenum. Sample MLQ 540, taken from the Alum Mine (Table 8), shows extremely low silica values, high total iron values, and anomalously high sulfur values. Fluorine content is high in rocks of the area, but Table 7 shows no correlation between U_3O_8 and fluorine.

Vanadium contents of the area are slightly higher than average contents for similar crustal rocks. The vanadium contents, the molybdenum contents, the hydrothermal alteration, and the numerous volcanic vents suggest that a pluton exists in the shallow subsurface.

Favorable criteria for the Alum Mountain area include the hydrothermal alteration of country rock, anomalously high vanadium, molybdenum, and fluorine contents and HSSR and ARMS anomalies. A potential uranium source is the silicic volcanic rocks from which uranium may have been leached by circulating ground water or by magmatic-hydrothermal fluids from the inferred pluton. Uranium precipitation may have been induced by temperature-pressure changes or by reduction by sulfides. Potential host rocks are altered volcanic flows.

Unfavorable criteria include the almost complete lack of uranium in the rocks. Chemical U_3O_8 values average 4 ppm and range from less than 1 ppm to 19 ppm. No radioactivity was observed in the field during traverses. The evidence is inconclusive, and the area therefore remains unevaluated.

CONTACT BETWEEN PALEOZOIC AND TERTIARY ROCKS

The contact between Paleozoic and Tertiary rocks is unevaluated because of the lack of subsurface data. Exposures of Paleozoic rocks are sparse

TABLE 7. Selected Chemical Values of the Alum Mountain Area

Sample no.	U_3O_8 (ppm)	V (ppm)	Mo (ppm)	Sample no.	U_3O_8 (ppm)	V (ppm)	Mo (ppm)
MLQ 029	2	295	27	MLQ 544		145	16
MLQ 030	3	224	19	MLQ 545	4	310	23
MLQ 031	3	226	17	MLQ 546	3	321	33
MLQ 032	6	231	27	MLQ 547	3	485	45
MLQ 033	6	139	21	MLQ 548	<1	123	16
MLQ 034	9	136	<10	MLQ 549	5	282	18
MLQ 035	5	304	33	MLQ 550	<1	161	30
MLQ 524	2	377	13	MLQ 551	1	<100	18
MLQ 525	2	260	15	MLQ 552	<1	126	16
MLQ 536	3	197	30	MLQ 553	4	142	22
MLQ 537	3	<100	20	MLQ 554	10	241	36
MLQ 538	5	160	23	MLQ 555	3	<100	19
MLQ 539	<1	144	26	MLQ 556	19	350	31
MLQ 540	<1	509	36	MLQ 557	3	210	17
MLQ 541	4	275	17	MLQ 558	<1	430	52
MLQ 542	6	167	21	MLQ 559	4	135	25
					$\bar{X}$ = 4	$\bar{X}$ = 227	$\bar{X}$ = 25

Correlation Coefficients: U_3O_8 vs V = 0.05; U_3O_8 vs Mo = 0.05; V vs Mo = 0.05; U_3O_8 vs total alkalies = 0.03; U_3O_8 vs Na_2O = 0.02; U_3O_8 vs F = 0.08

TABLE 8. Major oxide chemical data for the Alum Mountain Area

Sample no.	SiO_2	Al_2O_3	K_2O	MgO	Na_2O	CaO	Fe_2O_3	FeO	TiO_2	MnO	S	F (ppm)
MLQ 029	49.52	16.44	0.93	5.02	3.05	8.40	8.66	1.26	1.49	0.13	<0.01	---
MLQ 030	54.49	15.86	3.14	2.68	3.61	5.40	7.97	0.21	1.25	0.10	0.02	401
MLQ 031	60.39	12.76	2.29	1.77	1.25	3.47	3.79	<0.10	0.72	0.06	<0.01	<200
MLQ 032	57.59	15.44	3.77	2.68	3.52	3.74	3.03	0.58	0.80	0.08	<0.01	827
MLQ 033	64.71	13.62	4.40	0.19	3.17	0.24	0.92	<0.10	0.25	0.05	<0.01	271
MLQ 034	50.46	11.23	3.14	0.69	0.76	2.52	0.92	<0.10	0.22	0.06	<0.01	<200
MLQ 035	57.07	15.50	2.85	3.59	3.47	7.27	4.66	0.90	0.78	0.13	<0.01	528
MLQ 524	4.21	0.37	0.10	0.22	0.07	62.96	0.06	<0.10	0.04	0.01	<0.01	213
MLQ 525	70.48	11.53	3.46	0.91	1.32	3.60	1.73	<0.10	0.24	0.12	<0.01	233
MLQ 536	71.82	13.02	5.66	1.55	2.64	0.57	0.79	0.24	0.27	0.05	<0.01	234
MLQ 537	74.11	12.38	5.03	0.32	3.47	0.41	0.74	0.26	0.19	0.04	<0.01	256
MLQ 538	72.85	13.04	5.34	0.39	3.87	0.88	0.60	<0.10	0.19	0.05	<0.01	1302
MLQ 539	73.92	13.06	5.03	0.28	3.26	0.37	0.88	<0.10	0.17	0.06	0.09	266
MLQ 540	14.34	11.40	0.68	0.04	0.49	0.17	4.37	8.49	0.39	<0.01	15.20	---
MLQ 541	51.95	14.10	1.42	4.72	1.87	7.05	6.46	0.48	1.18	0.06	<0.01	2289
MLQ 542	72.84	14.15	4.71	0.24	3.19	0.24	0.89	0.18	0.22	0.04	<0.01	767
MLQ 544	70.01	13.74	5.03	0.41	3.87	1.19	1.22	<0.10	0.39	0.04	<0.01	444
MLQ 545	61.07	14.88	3.46	3.50	2.50	3.02	3.61	0.12	0.77	0.08	<0.01	---
MLQ 546	54.91	16.52	2.85	3.37	3.47	4.46	5.11	0.16	1.09	0.08	<0.01	---
MLQ 547	44.02	15.75	1.42	5.75	3.87	4.61	11.83	<0.10	1.10	0.17	<0.01	---
MLQ 548	79.74	22.72	4.07	0.12	3.87	0.11	0.62	<0.10	0.14	0.04	<0.01	---
MLQ 549	66.08	14.23	4.40	0.15	0.64	1.02	0.38	<0.10	0.11	0.03	<0.01	---
MLQ 550	73.92	12.87	4.40	0.22	3.87	0.31	1.01	0.20	0.25	0.06	<0.01	755
MLQ 551	76.12	11.72	4.07	0.16	3.87	0.33	0.71	0.16	0.25	0.06	<0.01	585
MLQ 552	64.65	15.23	3.46	0.62	4.92	2.66	1.65	0.30	0.42	0.08	<0.01	917
MLQ 553	72.66	11.94	4.07	0.22	3.87	0.23	0.76	0.10	0.21	0.05	0.01	434
MLQ 554	67.38	14.88	4.71	0.61	4.57	1.12	1.37	0.16	0.47	0.07	0.01	891
MLQ 555	71.96	11.86	4.07	0.19	3.87	5.80	0.19	0.25	0.17	0.06	0.01	551
MLQ 556	50.94	15.40	1.55	6.71	3.33	8.40	7.31	1.49	1.82	0.18	0.01	632
MLQ 557	51.76	11.34	2.17	1.28	1.73	0.44	2.99	0.46	0.72	0.06	0.01	479
MLQ 558	56.30	13.77	2.36	2.99	2.92	6.48	6.52	1.86	1.92	0.14	0.01	446
MLQ 559	69.51	14.15	4.34	0.13	3.87	0.30	0.65	0.21	0.21	0.04	0.01	250

Values in percent unless otherwise indicated.

within the Clifton Quadrangle (Pl. 7), and access to most of them was restricted. Distribution and lithologies of Paleozoic units are discussed under unfavorable environments. A discussion of Tertiary stratigraphy is in Appendix E.

Some indications of mineralization are given by HSSR data. Two groundwater anomalies are associated with the margins of the Mule Creek caldera (areas B-1 and B-2, Pl. 4). Another anomaly (area C, Pl. 4) was reported in stream and spring sediments along the Gila Cliff Dwellings caldera margin.

In this study, water samples were collected from five springs in the Bursum and Gila Cliff Dwellings calderas (App. B-1; Pl. 5a, 5b). Selected results are given in Table 9, as well as some average element and compound contents of ground water flowing through a rhyolite and of surface water of the world. Uranium will complex with sulfate or fluorine in an oxidizing environment in waters with a low pH. In waters with a high pH, uranium complexes with carbonate in oxidizing to slightly reducing environments. Samples MLQ 045 and 046 were taken near the resurgent dome of the Bursum caldera (Pl. 5a, 5b). Less than 1 ppb uranium is present in these samples; the sulfate and fluorine contents are low, and the carbonate content of MLQ 046 is high. From these data, there does not seem to have been any enrichment on the dome.

Samples MLQ 026, 027, and 028 (Pl. 5a, 5b) were collected along the margin of the Gila Cliff Dwellings caldera, the first two on the Middle Fork of the Gila River and the last near Alum Mountain. When the threshold value of 4 ppm uranium is used for anomalies, as it was in HSSR interpretation, the uranium contents of all three samples are anomalous. The calcium and fluorine contents of all three samples and the sulfate content of MLQ 026 and 028 are high.

The Bloodgood Canyon tuff is an aquifer in the region (Krier, 1980). If the springs that were sampled are flowing mainly from the tuff, the anomalous uranium content could be caused by leaching of the tuff. On the other hand, if the ground water is flowing from fractures along the caldera margins, these anomalous uranium values in waters of high sulfate, fluorine, and calcium contents may indicate the concentration of uranium at depth.

Gravimetric studies indicate that the Paleozoic section is present on the eastern side of the Gila Cliff Dwellings caldera and is present as a structural block under the Mogollon Mountains. Anomalies of beryllium, bismuth, gold, silver, copper, and molybdenum are associated with the margins of the calderas. Ratte and others (1979) postulated that the alteration present in the Gila Cliff Dwellings caldera is due to postcaldera hydrothermal activity and that in the Bursum caldera it is due to resurgence; this activity may have caused the remobilization of minerals formed during Laramide mineralization within the Paleozoic rocks.

UPPER NACO-LOWER SUPAI INTERVAL

The upper Naco-lower Supai interval is unevaluated because of insufficient evidence. Subsurface data are lacking and access to outcrops is restricted. The Naco Formation, of Pennsylvanian age, is divided into three

TABLE 9. Selected results from spring waters of the Bursum and Gila Cliff Dwelling calderas and average content of some elements and compounds in ground water in a rhyolite and surface waters.

	pH	U ppm	Ca ppm	Na ppm	SO_4 ppm	Cu ppb	Zn ppb	F ppm
Ground water in a rhyolite*	7.9	---	8.0	62000	22.0	---	---	---
Surface waters*	6.0-8.5	0.4	15.0	6300	11.2	7	20	0.1
Sample no. MLQ 026	7.6	4.0	17.0	144	78.0	2	6	9.0
Sample no. MLQ 027	8.3	5.0	17.0	41	14.0	2	5	5.0
Sample no. MLQ 028	8.4	5.0	22.0	141	69.0	15	2029	8.0
Sample no. MLQ 045	8.4	<1.0	6.0	---	3.0	3	---	<1.0
Sample no. MLQ 046	8.6	<1.0	15.0	---	13.0	2	---	<1.0

*Data from Levinson, 1980.

informal members, which, in ascending order, are the Alpha, Beta, and Gamma members (Brew, 1965). The Supai Formation, of Pennsylvanian-Permian age, is composed of four members which, in ascending order, are the Amos Wash Member, Big A Butte Member, Fort Apache Limestone, and Corduroy Member (Fig. 3a). The Alpha member, the lower half of the Beta member, the Big A Butte Member, and the Corduroy Member are discussed under unfavorable sandstone environments. The Fort Apache Limestone is discussed under unfavorable sandstone environments. Only the upper half of the Beta member, the Gamma member, and the Amos Wash Member are known to have favorable characteristics outside the study area.

The upper half of the Beta member is composed of repeated sequences of limestone and noncalcareous units of shale, mudstone, and shaly siltstone. Conformably overlying the Beta member, the Gamma member is composed of reddish mudstone, laminated and cross-bedded siltstone, and fine-grained sandstone with minor limestone and conglomerate (Brew, 1965). The contact of the Naco Formation and Supai Formation is gradational and time transgressive (Brew, 1965; Winters, 1963). The Amos Wash Member of the Supai Formation is composed of alternating red-brown, noncalcareous, fine-grained sandstone, siltstone, and mudstone. The Amos Wash Member is conformably overlain by the Big A Butte Member (Winters, 1963).

The Supai Formation was deposited in a prograding delta that advanced from north to south (Winters, 1963). The northern facies of the delta were deposited at the same time as the upper facies of the Naco Formation. These northern deltaic deposits and the Kaibab uplift were possible sources for the detritus of the Naco Formation (Brew, 1965). The Uncompahgre-San Luis uplift and the Zuni-Defiance uplift were probably sources for the detritus of the Supai Formation (Winters, 1962, 1963). The sediments of both formations were deposited in environments fluctuating from continental to marine (Brew, 1965; Winters, 1963).

Peirce and others (1976) described the zone of contact between the two formations where it is exposed along the Mogollon Rim west of the Clifton Quadrangle (Fig. 2). Local carbonaceous trash and lignites are reported (McGoon, 1962; Romers, 1977). Uranium concentration is associated with these reductants in channel-controlled peneconcordant (Subclass 243) and non-channel-controlled peneconcordant (Subclass 244) uranium occurrences (Peirce and others, 1976; McGoon, 1962; Rogers, 1977). Copper, lead, and zinc sulfide and copper oxide mineralization are also found locally (Peirce and others, 1976). Peirce and others (1976) postulated the Zuni-Defiance uplift as a source of the uranium.

Outcrops of this zone in the Clifton Quadrangle are present only within the Fort Apache Indian Reservation, to which access is restricted. No subsurface data are available. Therefore, the interval remains unevaluated.

BACA FORMATION

The Baca Formation in New Mexico and the Eager Formation in Arizona are unevaluated within the Clifton Quadrangle because of the lack of subsurface data and outcrops. The two formations are correlative and will be referred to as the Baca Formation in the following discussion.

During the Eocene and Early Oligocene, the Baca Formation was deposited in a series of fluvial and lacustrine facies. Humid, alluvial fans were deposited from the Mogollon Highlands and the Zuni-Defiance uplift (Fig. 2). At the base of the fans, a fluvial meander belt developed. The streams deposited their detritus in lacustrine delta facies within a shallow lake (Johnson, 1978). The formation consists of interbedded and interfingering red sandstone, conglomerate, siltstone, and greenish shale (Fig. 3c).

North and northeast of the New Mexico half of the Clifton Quadrangle the Baca Formation unconformably overlies the Cretaceous Mesaverde Formation. Several uranium occurrences are known near the contact of these formations; the Red Basin claims in sec. 19 and 20, T. 2 N., R. 10 W., are the best documented. Concentration is located in a stream channel of the Baca Formation confined between an overlying shale and an underlying shale of the Mesaverde Formation. Uranium from circulating ground water was probably reduced by carbonaceous trash within the permeable sandstone of the stream channel (Anonymous, 1959). The overlying Tertiary volcanics are the probable source of uranium. It is possible that similar deposits related to differential permeability and unconformities could occur within the Baca Formation in the subsurface of the Clifton Quadrangle.

GILA CONGLOMERATE

The Gila Conglomerate is unevaluated because of lack of subsurface data. Within the Clifton Quadrangle, the name Gila Conglomerate (Fig. 3c) is given to the numerous basin deposits of Miocene to Pleistocene age (Elston, 1976). The formation consists of conglomerate, sandstone, siltstone, claystone, and mudstone interbedded with local andesitic to basaltic lava flows. Volcanic debris and tuffaceous sediments form part of the clastics. The rocks were deposited in alluvial, fluvial, playa, and lacustrine environments (Heindl, 1958) within trenches bounded by cauldrons (Pl. 9). Climate ranged from semiarid to semihumid (Heindl, 1958). Thickness of the formation is unknown, but may exceed 1525 m (Coney, 1976).

Unfavorable characteristics of the Gila include the lack of reductants or well-developed channeling on outcrop. The reddish color of the rocks indicates an oxidizing environment. Samples MLQ 505 and 519, taken from the same outcrop, have chemical uranium values of 26 ppm and 1 ppm, respectively (Pl. 5a, 5b; App. B-1). Uranium has probably been released from allogenic feldspars, volcanic debris, or tuffaceous sediments, but the lack of reductant has precluded the concentration of uranium. No ARMS anomalies are known in the Gila.

Favorable characteristics include excellent sources of uranium in the rhyolites in the ash-flow tuffs of the surrounding cauldrons, and in the volcanic debris, which is a major constituent of the formation. The Gila is the primary aquifer within the basins (Heindl, 1958). An HSSR anomaly was found in ground water of the Mangus Trench (area B-2, Pl. 4). Tuffaceous lacustrine sediments (MLQ 513 and 054, App. D, Pl. 5a) are located in the Mangus Trench and San Agustin Plains (Pl. 9). Zeolites reported within these beds (Ratte and Finnel, 1978), clays, or preserved carbonaceous trash could serve as concentrating mechanisms within a reducing environment below the water table.

INTERPRETATION OF AERIAL RADIOMETRIC DATA

Texas Instruments, Inc. (1978), identified 265 first-priority radiometric anomalies. Of these, 146 were recommended for field checking. The latter were selected on the basis of their statistical significance and their locations on the geologic map (Pl. 7).

A statistically significant anomaly does not necessarily represent mineralized rock. The authors outlined six areas (Pl. 3) where uranium count rates are in the upper 10 percent of the range of count rates for the Clifton Quadrangle. These areas are discussed below. Although these areas represent the highest radioactivity in the Clifton Quadrangle, they are below values indicative of uranium provinces.

Area A is in volcanic rocks of the Gila and the Bursum calderas. The cauldron fill consists of ash-flow tuff of the high-silica alkali-rhyolite suite. Field checking in this area indicated that uranium was widely dispersed because of the pyroclastic nature of eruption. Anomalous radioactivity was not observed on the ground.

Area B is along the ring-fracture system of the Bursum caldera. Rock types include ash-flow tuff, rhyolite and quartz latite flows and domes, volcaniclastic detritus, and andesitic flows and dikes. These belong to both the calc-alkalic and high-silica alkali-rhyolite suite. Area B coincides with favorable Area A (Pl. 1).

Area C is northeast of Datil, New Mexico, and north of the San Agustin Plains. Rock types are predominantly rhyolitic ash-flow tuff and quartz latitic to rhyolitic flows with interbedded volcaniclastic detritus. Ground searches failed to recognize anomalous radioactivity.

Area D is on the southern border of the quadrangle, near the Arizona-New Mexico state line. The area outlines the Mule Creek caldera. Ground traverses failed to define anomalous radioactivity in the area. The aerial response is probably due to the interbedded rhyolitic and ash-flow-tuff units of the caldera.

Area E, in the southwest corner of the quadrangle, is in Precambrian metasedimentary rocks, Tertiary volcanic rocks, and Quaternary alluvium. Ground checking did not reveal areas of anomalous radioactivity. The apparent aerial anomaly may be due to contrasting rock types that yield erroneous apparent anomalies.

INTERPRETATION OF HYDROGEOCHEMICAL AND STREAM-SEDIMENT RECONNAISSANCE

Hydrogeochemical and stream-sediment sampling of the New Mexico half of the Clifton Quadrangle was performed by the Los Alamos Scientific Laboratory (Sharp and others, 1978). Samples were analyzed for chemical uranium content. The four areas of anomalous uranium content (Pl. 4) are associated with high-silica, rhyolitic calderas.

Uranium content in surface waters of the world averages 0.4 ppb uranium (Levinson, 1980). To correct for any high uranium values caused by unusually high dissolved-solids content in the water, the uranium values were first divided by conductivity; then they were multiplied by 100 to give a more manageable number. In the present study, anomalously high surface-water uranium contents are those over a threshold value of 4.0 ppb. One anomalous sample, collected in the West Fork of Mogollon Creek (Pl. 4, 13), has a value of 5.4 ppb uranium. The drainage system of the West Fork flows primarily through the Apache Springs Quartz Latite, which is the tuffaceous cauldron fill of the Bursum caldera. Rock samples MLQ 581 and MLQ 583 from the same area have chemical uranium values of 3 ppb (Pl. 5a, 5b; App. B-1). The slightly high uranium value of the ground water is probably due to leaching of the overlying tuff.

From ground-water sample analyses, two areas, B-1 and B-2, were recognized as anomalous when compared to the threshold value of 4.0 ppb uranium (Pl. 4). In both areas, maximum uranium concentrations are greater than 10 ppb. The areas are associated with the margins of the Mule Creek caldera (Pl. 9). Uranium in the water may have been leached from the high-silica, rhyolitic domes and flows of the caldera.

Most of the sediment samples are from drainage systems through felsic rocks. As the average uranium content of felsic rocks of the world is 4.8 ppm (Levinson, 1980), a threshold value of 10 ppm was chosen, in the present study, to delineate anomalous areas. Area C (Pl. 4) was found to be anomalous. This area is in the Gila River drainage system, where it primarily flows through the center and margins of the Gila Cliff Dwellings caldera.

Of the three samples in area C with uranium values greater than 10 ppm, two are wet sediments from springs found on the ring-fracture system. Uranium values from these samples are 10.7 ppm and 17.2 ppm (Sharp and others, 1978). Uranium, in waters rising from depth, could have been precipitated in these two sediments by the changing of the oxidation state of uranium species and by pressure differences. The third sample is of dry sediments collected from where the drainage runs through the center of the caldera. There the stream drains the Bloodgood Canyon Rhyolite, the tuffaceous cauldron fill of the Gila Cliff Dwellings caldera. The uranium content of the sample is 10.2 ppm (Sharp and others, 1978). Rock samples from the area average 3.2 ppm cU_3O_8 (MLQ 524, 526, and 537; Pl. 5a, 5b; App. B-1). The anomalous uranium value may be due to concentration of uranium in heavy minerals, which were not separated from the sample. Alternately, uranium leached from nearby tuff may have been concentrated in the sediments by evaporation.

RECOMMENDATIONS TO IMPROVE EVALUATION

It is recommended that two areas be studied more thoroughly. These areas are Alum Mountain in the Gila Wilderness and Red Mountain in the Blue Range Wilderness. The general geology, favorable data, and conflicting data are described in the unevaluated environments section of this report.

In both the Alum Mountain area and the Red Mountain area, access is a problem, and, thus, sampling and regional studies are difficult. Therefore,

it is recommended that 10 man-days be allocated to each of these areas. The work would require horsepack trips. Rock sampling and gamma-ray spectrometric measuring would help in the interpretation of the conflicting evidence so that favorability evaluation may be completed.

SELECTED BIBLIOGRAPHY

Aldrich, M. J., Jr., 1976, Geology and flow directions of volcanic rocks of the North Star Mesa Quadrangle, Grant County, New Mexico, in Elston, W. E., and Northrop, S. A., eds., Cenozoic volcanism in southwestern New Mexico: New Mexico Geological Society Special Publication 5, p. 79-81.

Anonymous, 1959, Uranium deposits in the Datil Mountains, Bear Mountains region, New Mexico, in Weir, J. E., Jr., and Baltz, E. H., eds., Guidebook of west-central New Mexico: New Mexico Geological Society 10th Field Conference, p. 135-143.

Arizona Bureau of Mines, 1962a, Map of outcrops of Tertiary and Quaternary igneous rocks in Arizona: Arizona Bureau of Mines, scale 1:1,000,000.

-----1962b, Map of outcrops of Paleozoic and Mesozoic rock in Arizona: Arizona Bureau of Mines, scale 1:1,000,000.

Armstrong, A. K., 1959, Mississippian strata on the eastern side of the Datil Plateau, in Weir, J. E., Jr., and Baltz, E. H., eds., Guidebook of west-central New Mexico: New Mexico Geological Society 10th Field Conference, p. 52-56.

Austin, Ralph, and D'Andrea, R. F., Jr., 1978, Sandstone-type uranium deposits in Mickle, D. G., and Mathews, G. W., eds., Geologic characteristics of environments favorable for uranium deposits: U.S. Department of Energy Open-File Report GJBX-67(78), p. 87-120.

Brew, D. C., 1965, Stratigraphy of the Naco Formation (Pennsylvanian) in Central Arizona: Ithaca, New York, Cornell University, Ph.D. dissertation, 201 p.

Bryant, D. L., 1968, Diagnostic characteristics of the Paleozoic formations of southeastern Arizona, in Titley, S. R., ed., Southern Arizona Guidebook III, 1968: Arizona Geological Society, p. 33-47.

Burnham, C. W., 1959, Metallogenic provinces of the southwestern United States and northern Mexico: New Mexico Bureau of Mines and Mineral Resources Bulletin 65, 76 p.

Chapin, C. E., Chamberlin, R. M., Osborn, G. R., White, D. L., and Sanford, A. R., 1978, Exploration framework of the Socorro geothermal area, New Mexico, in Chapin, C. E., and Elston, W. E., eds., Field guide to selected cauldrons and mining districts of the Datil-Mogollon volcanic field, New Mexico: New Mexico Geological Society Special Publication 7, p. 115-130.

Collins, G. E., 1957, Reconnaissance for uranium in the Mogollon mining district, Catron County, New Mexico: U.S. Atomic Energy Commission Technical Memorandum Report DAO-4-TM-7, 26 p.

Condie, K. C., and Budding, A. J. 1979, Geology and geochemistry of Precambrian rocks, central and south-central New Mexico: New Mexico State Bureau of Mines and Mineral Resources Memoir 35, 58 p.

Coney, P. J., 1976, Structure, volcanic stratigraphy, and gravity across the Mogollon Plateau, New Mexico, in Elston, W. E., and Northrop, S. A., eds., Cenozoic volcanism in southwestern New Mexico: New Mexico Geological Society Special Publication 5, p. 29-41.

Dane, C. H., and Bachman, G. O., 1961, Preliminary geologic map of the southwestern part of New Mexico: U.S. Geological Survey Miscellaneous Geologic Investigations Map I-344, scale 1:380,160.

-----1965, Geologic map of New Mexico: U.S. Geological Survey, scale 1,500,000, 2 sheets.

Deal, E. G., and Rhodes, R. C., 1976, Volcano-tectonic structures in the San Mateo Mountains, Socorro County, New Mexico, in Elston, W. E., and Northrop, S. A., eds., Cenozoic volcanism in southwestern New Mexico: New Mexico Geological Society Special Publication 5, p. 51-57.

Doe, B. R., Steven, T. A., Delevaux, M. H., Stacey, J. S., Lipman, P. W., and Fisher, F. S., 1979, Genesis of ore deposits in the San Juan volcanic field, southwestern Colorado--lead-isotope evidence: Economic Geology, v. 74, p. 1-27.

Elston, W. E., 1957, Geology and mineral resources of Dwyer Quadrangle, Grant, Luna, and Sierra Counties, New Mexico: New Mexico State Bureau of Mines and Mineral Resources Bulletin 38, 86 p.

-----1976, Glossary of stratigraphic terms of the Mogollon-Datil volcanic province, New Mexico, in Elston, W. E., and Northrop, S. A., eds., Cenozoic volcanism in southwestern New Mexico: New Mexico Geological Society Special Publication 5, p. 131-144.

-----1978, Mid-Tertiary cauldrons and their relationships to mineral resources, southwestern New Mexico: A brief review, in Chapin, C. E., and Elston, W. E., eds., Field guide to selected cauldrons and mining districts of the Datil-Mogollon volcanic field, New Mexico: New Mexico Geological Society Special Publication 7, p. 107-113.

Elston, W. E., Coney, P. J., and Rhodes, R. C., 1968, A progress report on the Mogollon Plateau volcanic province, southwestern New Mexico: Colorado School of Mines Quarterly, v. 63, p. 261-287.

Elston, W. E., Damon, P. E., Coney, P. J., Rhodes, R. C., Smith, E. I., and Bikerman, Michael, 1973, Tertiary volcanic rocks, Mogollon-Datil province, New Mexico and surrounding region; K-Ar dates, patterns of eruption, and periods of mineralization: Geological Society of America Bulletin, v. 84, p. 2259-2274.

Flower, R. H., 1965, Early Paleozoic of New Mexico, in Fitzsimmons, J. P., and Lochman-Balk, Christina, eds., Southwestern New Mexico II: New Mexico Geological Society Guidebook, 16th Field Conference, p. 112-131.

Foster, R. W., 1964, Stratigraphy and petroleum possibilities of Catron County, New Mexico: New Mexico State Bureau of Mines and Mineral Resources Bulletin 85, 55 p.

Gillerman, Elliot, 1964, Mineral deposits of western Grant County, New Mexico: New Mexico Bureau of Mines and Mineral Resources Bulletin 83, 213 p.

Hahman, W. R., Sr., Stone, C., and Witcher, J. C., 1978, Preliminary map, geothermal energy resources of Arizona: Arizona Bureau of Geology and Mineral Technology Geothermal Map 1, scale 1:1,000,000.

Hayes, P. T., 1970, Cambrian and Ordovician rocks of southeastern Arizona and southwestern New Mexico, in Callender, J. F., Wilt, J. C., and Clemons, R. E., eds., Land of Cochise, southeastern Arizona: New Mexico Geological Society Guidebook, 29th Field Conference, p. 165-173.

Heindl, L. A., 1958, Cenozoic alluvial deposits of the upper Gila River area, New Mexico and Arizona: Tucson, University of Arizona, Ph.D. dissertation, 249 p.

Huddle, J. W., and Dobrovolny, Ernest, 1952, Devonian and Mississippian rocks of central Arizona: U.S. Geological Survey Professional Paper 233-D, p. 67-112.

Hunt, C. B., 1978, Surficial geology of southwest New Mexico: New Mexico State Bureau of Mines and Mineral Resources Geological Map 42, scale 1:500,000.

Jones, C. A., 1978, Uranium occurrences in sedimentary rocks exclusive of sandstone, in Mickle, D. G., and Mathews, G. W., eds., Geologic characteristics of environments favorable for uranium deposits: U.S. Department of Energy Open-File Report GJBX-67(78), p. 1-86.

Johnson, B. D., 1978, Genetic stratigraphy and provenance of the Baca Formation, New Mexico, and the Eagar Formation, Arizona: Austin, University of Texas, M.A. thesis, 150 p.

Kottlowski, F. E., 1963, Paleozoic and Mesozoic strata of southwestern and south-central New Mexico: New Mexico State Bureau of Mines and Mineral Resources Bulletin 79, 100 p.

Krier, D. J., 1980, Geology of the southern part of the Gila Primitive Area, Grant County, New Mexico: Albuquerque, University of New Mexico, M.S. thesis, 113 p.

Levinson, A. A., 1980, Introduction to exploration geochemistry: Wilmette, Illinois, Applied Publishing, Ltd., 924 p.

Lindgren, Waldemar, 1905, Description of the Clifton Quadrangle: U.S. Geological Survey Folio 129, 13 p.

Lochman-Bald, Christina, 1965, Lexicon of stratigraphic names used in southwestern New Mexico, in Fitzsimmons, J. P., and Lochman-Balk, Christina, eds., Southwestern New Mexico II: New Mexico Geological Society Guidebook, 16th Field Conference, p. 93-111.

McGoon, D. O., Jr., 1962, Occurrences of Paleozoic carbonaceous deposits in the Mogollon Rim region, in Weber, R. H., and Peirce, H. W., eds., Mogollon Rim region, east-central Arizona: New Mexico Geological Society Guidebook, 13th Field Conference, p. 89-91.

McKee, E. D., 1938, Environment and history of the Toroweap and Kaibab Formations of northern Arizona and southern Utah: Carnegie Institute of Washington Publication 492, 268 p.

McKee, E. D., and Gutschick, R. C., 1969, History of the Redwall Limestone in northern Arizona: Geological Society of America Memoir 114, p. 1-172.

Merrill, R. K., 1974, The late Cenozoic geology of the White Mountains, Apache County, Arizona: Tempe, Arizona State University, Ph.D. dissertation, 202 p.

Merrill, R. K., and Pewe, T. L., 1977, Late Cenozoic geology of the White Mountains, Arizona: Arizona Bureau of Geology and Mineral Technology Special Paper 1, 65 p.

Mickle, D. G., ed., 1978, A preliminary classification of uranium deposits: U.S. Department of Energy Open-File Report GJBX-63(78), 77 p.

Mickle, D. G., and Mathews, G. W., 1978, Geologic characteristics of environments favorable for uranium deposits: U.S. Department of Energy Open-File Report GJBX-67(78), 250 p.

Moore, R. T., 1968, Mineral deposits of the Fort Apache Indian Reservation, Arizona: Arizona Bureau of Mines Bulletin 177, 84 p.

Peirce, H. W., 1973, Geologic Guidebook 2--Highways of Arizona, Arizona Highways 77 and 177: Arizona Bureau of Mines Bulletin 17a, 73 p.

Peirce, H. W., Jones, Nile, and Rogers, Ralph, 1976, A survey of uranium favorability of Paleozoic rocks in the Mogollon Rim and slope region, east-central Arizona: Arizona Bureau of Geology and Mineral Technology Circular 19, 60 p.

Peirce, H. W., Keith, S. B. and Wilt, J. C., 1970, Coal, oil, natural gas, helium, and uranium in Arizona: Arizona Bureau of Mines Bulletin 182, p. 108-289.

Pilcher, R. C., 1978, Volcanogenic uranium occurrences, in Mickle, D. G., and Mathews, G. W., eds., Geologic characteristics of environments favorable for uranium deposits: U.S. Department of Energy Open-File Report GJBX-67(78), p. 181-220.

Ratte, J. C., 1980, Geologic map of the Saliz Pass Quadrangle, New Mexico: U.S Geological Survey Miscellaneous Field Studies Map MF-1203, scale 1:24,000.

Ratte, J. C., and Finnell, T. L., 1978, Third day road log from Silver City to Reserve via Glenwood and the Mogollon mining district, in Chapin, C. E., and Elston, W. E., eds., Field guide to selected cauldrons and mining districts of the Datil-Mogollon volcanic field, New Mexico: New Mexico Geological Society Special Publication 7, p. 49-63.

Ratte, J. C., and Gaskill, D. L., 1975, Reconnaissance geologic map of the Gila Wilderness study area, southwestern New Mexico: U.S. Geological Survey Miscellaneous Investigation Series Map I-886, scale 1:62,500, 2 sheets.

Ratte, J. C., Gaskill, D. L., Eaton, G. P., Peterson, D. L., Stotelmeyer, R. B., and Meeves, H. C., 1979, Mineral resources of the Gila Primitive Area and Gila Wilderness, New Mexico: U.S. Geological Survey Bulletin 1251, 229 p.

Ratte, J. C., Landis, E. R., Gaskill, D. L., and Raabe, R. G., 1969, Mineral resources of the Blue Range Primitive area, Greenless County, Arizona, and Catron County, New Mexico, with a section on aeromagnetic interpretation by G. P. Eaton: U.S. Geological Survey Bulletin 1261-E, 91 p.

Rhodes, R. C., 1976a, Volcanic geology of the Mogollon Range and adjacent areas, Catron and Grant Counties, New Mexico, in Elston, E. W., and Northrop, S. A., eds., Cenozoic volcanism in southwestern New Mexico: New Mexico Geological Society Special Publication 5, p. 42-50.

-----1976b, Petrologic framework of the Mogollon Plateau volcanic ring complex, New Mexico--surface exporession of a major batholith, in Elston, W. E., and Northrop, S. A., eds., Cenozoic volcanism in southwestern New Mexico: New Mexico Geological Society Special Publication 5, p. 103-112.

Rhodes, R. C., and Smith, E. I., 1973, Geology and tectonic setting of the Mule Creek caldera, New Mexico, U.S.A.: Bulletin volcanologique, v. 36, no. 3, p. 1-11.

-----1976, Stratigraphy and structure of the northwestern part of the Mogollon Plateau volcanic province, Catron County, New Mexico, in Elston, W. E., and Northrop, S. A., eds., Cenozoic volcanism in southwestern New Mexico: New Mexico Geological Society Special Publication 5, p. 57-62.

Rogers, R. D., 1977, Copper mineralization in Pennsylvanian-Permian rocks of the Tonto Rim segment of the Mogollon Rim in central Arizona: Tucson, University of Arizona, M.S. thesis, 65 p.

Ross, C. A., 1973, Pennsylvanian and early Permian depositional history, southeastern Arizona: American Association of Petroleum Geologists Bulletin, v. 57, no. 5, p. 887-912.

-----1978, Pennsylvanian and early Permian depositional framework, southeastern Arizona, in Callender, J. F., Wilt, J. C., and Clemons, R. E., eds., Land of Cochise, southeastern Arizona: New Mexico Geological Society in cooperation with Arizona Geological Society Guidebook, 29th Field Conference, p. 193-200.

Ruhe, R. V., 1967, Geomorphic surfaces and surficial deposits in southern New Mexico: New Mexico Bureau of Mines and Mineral Resources Memoir 18, 66 p.

Scarborough, R. B., and Wilt, J. C., 1979, A study of uranium favorability of Cenozoic sedimentary rocks, Basin and Range Province, Arizona; Part I, General geology and chronology of Pre-Late Miocene Cenozoic sedimentary rocks: U.S. Geological Survey Open-File Report 79-1,429, 101 p.

Schilling, C. H., and Schilling, J. H., 1961, Bibliography of New Mexico geology and mineral technology 1956-1960: New Mexico State Bureau of Mines and Mineral Resources Bulletin 74, 124 p.

Sharp, R. R., Jr., Morris, W. A., and Aamodt, P. L., 1978, Uranium hydrogeochemical and stream-sediment reconnaissance data release for the New Mexico portions of the Douglas, Silver City, Clifton, and Saint Johns NTMS Quadrangles, New Mexico/Arizona: U.S. Department of Energy Open-File Report GJBX-69(78), 123 p.

Smith, E. I., Aldrich, M. J., Deal, E. G., and Rhodes, R. C., 1976, Structural and petrology of the John Kerr Peak dome complex, southwestern New Mexico, in Elston, W. E., and Northrop, S. A., eds., Cenozoic volcanism in southwestern New Mexico: New Mexico Geological Society Special Publication 5, p. 71-78.

Smith, R. L., and Bailey, R. A., 1968, Resurgent cauldrons: Geological Society of America Memoir 116, p 613-662.

Stearns, C. E., 1962, Geology of the north half of the Pelona Quadrangle, Catron County, New Mexico: New Mexico State Bureau of Mines and Mineral Resources Bulletin 78, 46 p.

Strangway, D. W., Simpson, J., and York, Derek, 1976, Paleomagnetic studies of volcanic rocks from the Mogollon Plateau area of Arizona and New Mexico, in Elston, W. E., and Northrop, S. A., eds., Cenozoic volcanism in southwestern New Mexico: New Mexico Geological Society Special Publication 5, p. 119-125.

Summers, W. K., 1979, Hydrothermal anomalies in New Mexico: New Mexico State Bureau of Mines and Mineral Resources Map 1, scale 1:1,000,000.

Teichert, Curt, 1965, Devonian rocks and paleogeography of central Arizona: U.S. Geological Survey Professional Paper 464, 181 p.

Texas Instruments, Inc., 1978, Aerial radiometric and magnetic reconnaissance survey of portions of Arizona-New Mexico, Clifton Quadrangle: U.S. Department of Energy Open-File Report GJBX-23(79), v. 2-B, p. N1-H-54.

Thorman, C. H., 1977, Geologic map of the Coyote Peak and Brockman Quadrangles, Hidalgo and Grant Counties, New Mexico: U.S. Geological Survey Miscellaneous Field Studies Map MF-924, scale 1:48,000.

Trauger, F. D., 1972, Water resources and general geology of Grant County, New Mexico: New Mexico State Bureau of Mines and Mineral Resources Hydrologic Report 2, 211 p.

U.S. Geological Survey, 1972, Aeromagnetic map of the Morenci-Monticello area, southeastern Arizona and southwestern New Mexico: U.S. Geological Survey Geophysical Investigations Map GP-838, scale 1:250,000.

U.S. Geological Survey, Arizona Bureau of Mines, and the U.S. Bureau of Land Reclamation, 1975, Mineral and water resources of Arizona: Arizona Bureau of Mines Bulletin 180, 638 p.

Vuich, J., 1974, Strata-bound sulfide deposits and suggestions for exploration in Arizona: Arizona Bureau of Mines Circular 16, 11 p.

Wahl, D. E., Jr., 1980, Mid-Tertiary volcanic geology in parts of Greenless County, Arizona, Grant and Hidalgo Counties, New Mexico: Tempe, Arizona State University, Ph.D. dissertation, 149 p.

Weber, R. H., and Bassett, W. A., 1963, K-Ar ages of Tertiary volcanic and intrusive rocks in Socorro, Catron, and Grant Counties, New Mexico, in Kuellmer, F. J., eds., Guidebook of the Socorro region, New Mexico Geological Society Guidebook, 14th Field Conference, p. 220-223.

Weber, R. H., and Willard, M. E., 1959a, Reconnaissance geologic map of Reserve Thirty-Minute Quadrangle: New Mexico State Bureau of Mines and Mineral Resources Geologic Map 12, 1:126,720.

-----1959b, Reconnaissance geologic map of Mogollon Thirty-Minute Quadrangle: New Mexico State Bureau of Mines and Mineral Resources Geologic Map 10, scale 1:128,720.

Willard, M. E., Weber, R. H., and Kuellmer, Frederick, 1961, Reconnaissance geologic map of Alum Mountain Thirty-Minute Quadrangle: New Mexico State Bureau of Mines and Mineral Resources Geologic Map 13, scale 1:126,720.

Wilson, E. D., 1976, A resume of the geology of Arizona: Arizona Bureau of Mines Bulletin 171, 140 p.

Wilson, E. D., and Moore, R. T., 1958, Geologic map of Graham and Greenlee Counties, Arizona: Arizona Bureau of Mines, scale 1:375,000.

Wilson, E. D., Moore, R. T., and O'Haire, R. T., 1960, Geologic map of Navajo and Apache Counties, Arizona: Arizona Bureau of Mines, scale 1:375,000.

Wilson, E. D., O'Haire, R. T., and McCrory, F. J., 1961, Map and index of Arizona mining districts: Arizona Bureau of Mines, scale 1:1,000,000.

Winchester, D. E., 1920, Geology of Alamosa Creek Valley, Socorro County, New Mexico, with special reference to the occurrence of oil and gas: U.S. Geological Survey Bulletin 716, p. 1-15.

Winters, S. S., 1962, Lithology and stratigraphy of the Supai Formation, Fort Apache Indian Reservation: in Weber, R. H., and Peirce, H. W., eds., Mogollon Rim region, east-central Arizona: New Mexico Geological Society Guidebook, 13th Field Conference, p. 87-88.

-----1963, Supai Formation (Permian) of eastern Arizona: Geological Society of America Memoir 89, 99 p.

Wrucke, C. T., 1961, Paleozoic and Cenozoic rocks in the Alpine-Nutrioso area, Apache County, Arizona: U.S. Geological Survey Bulletin 1,121-H, 26 p.

CLIFTON, ARIZONA/ NEW MEXICO

EXPLANATION

URANIUM OCCURRENCES

	CLASSIFICATION			
	Sedimentary	Plutonic	Volcanic	Other
Minor prospect or mineral occurrence	□	△	⬠	☼
Significant prospect or mine reporting minor production	◪	▲	◑	✱
Mine having production over 200,000 pounds U_3O_8	■	▲	⬟	✹
Not visited	□Y	△Y	⬠Y	☼Y
Not found	□X	△X	⬠X	☼X
Mining District				

URANIUM RESOURCE EVALUATION
ISSUED BY THE U.S. DEPARTMENT OF ENERGY

5 0 5 10 15 20 25 MILES

5 0 5 10 15 20 25 KILOMETERS

BASE MAP CONTROL FROM USGS

Plate 2. URANIUM OCCURRENCES

February 1981
Plate 2.

CLIFTON, ARIZONA/ NEW MEXICO

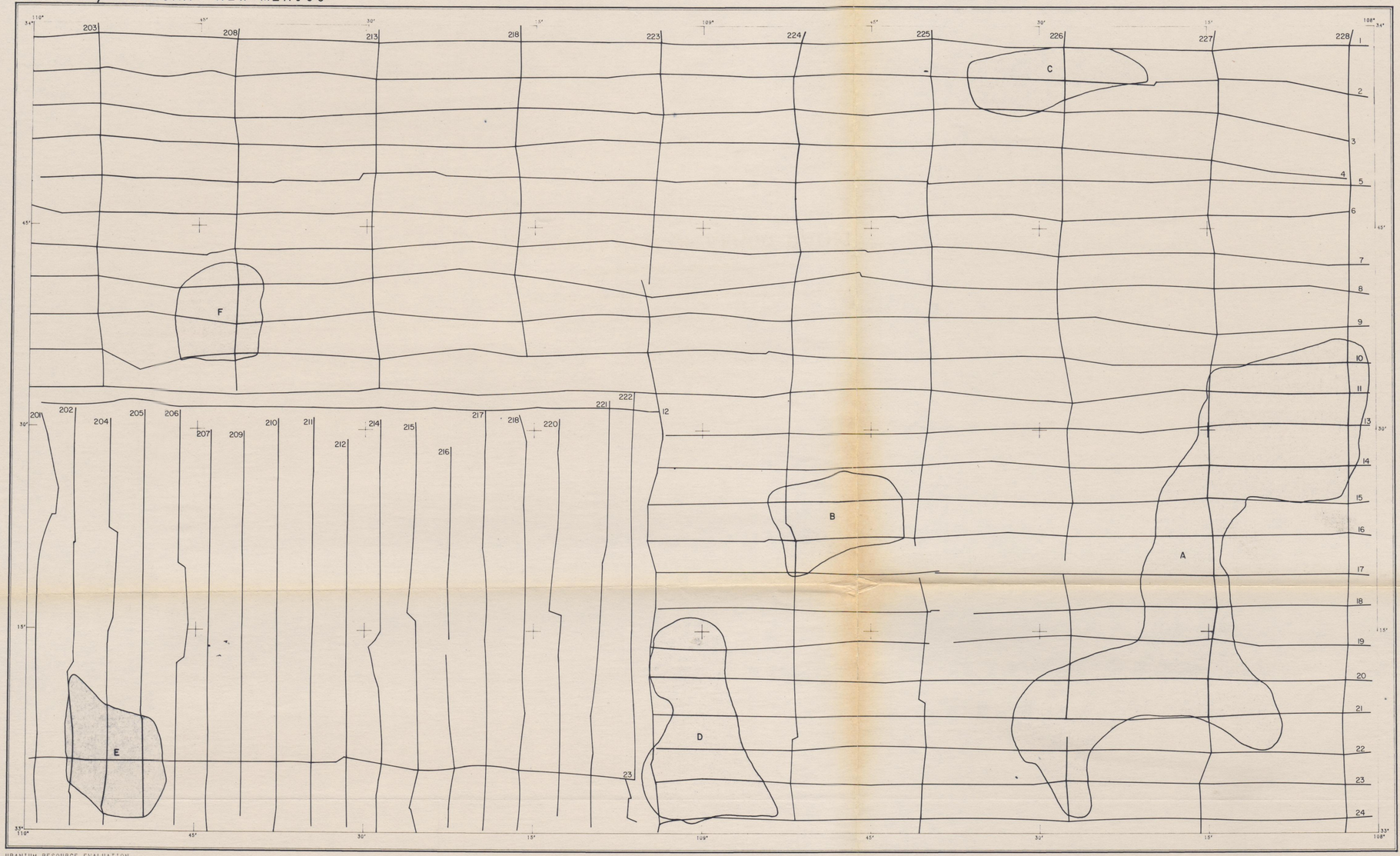

URANIUM RESOURCE EVALUATION
ISSUED BY THE U.S. DEPARTMENT OF ENERGY

5 0 5 10 15 20 25 MILES

5 0 5 10 15 20 25 KILOMETERS

BASE MAP CONTROL FROM USGS
DATA SOURCE: TEXAS INSTRUMENTS INC., 1978

EXPLANATION

AERIAL RADIOMETRIC DATA

223
—10— Flightline and number

Anomalous areas detected by aerial radiometric survey

Plate 3. INTERPRETATION OF AERIAL RADIOMETRIC DATA

February 1981
Plate 3.

CLIFTON, ARIZONA/ NEW MEXICO

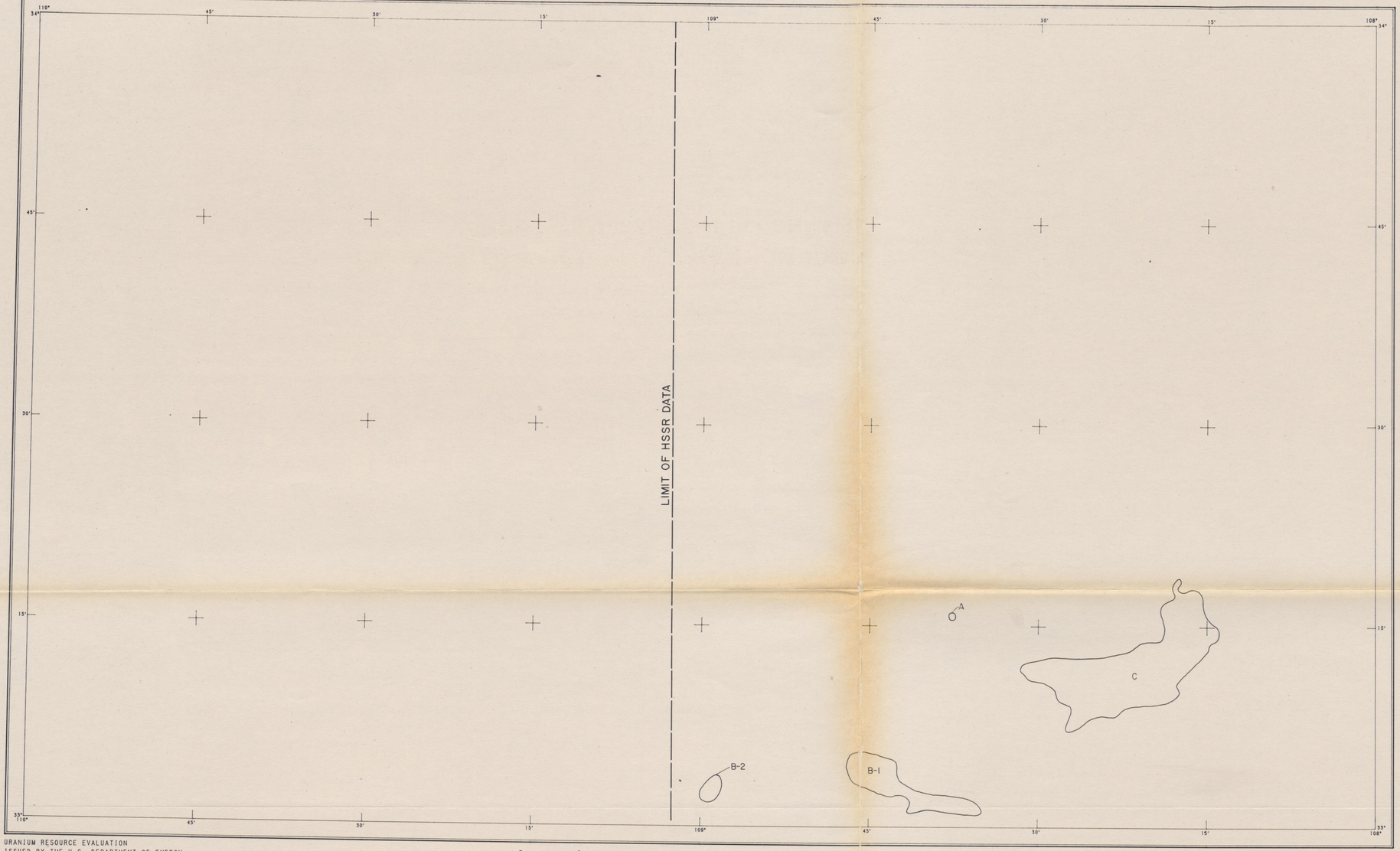

EXPLANATION

Areas of greater than threshold value concentration.

A Surface water anomaly

B Ground water anomaly

C Sediment anomaly

URANIUM RESOURCE EVALUATION
ISSUED BY THE U.S. DEPARTMENT OF ENERGY

5 0 5 10 15 20 25 MILES

5 0 5 10 15 20 25 KILOMETERS

BASE MAP CONTROL FROM USGS
DATA SOURCE: SHARP & OTHERS, 1978

Plate 4. INTERPRETATION OF DATA FROM HYDROGEOCHEMICAL AND STREAM-SEDIMENT RECONNAISSANCE

February 1981
Plate 4.

CLIFTON, ARIZONA/ NEW MEXICO

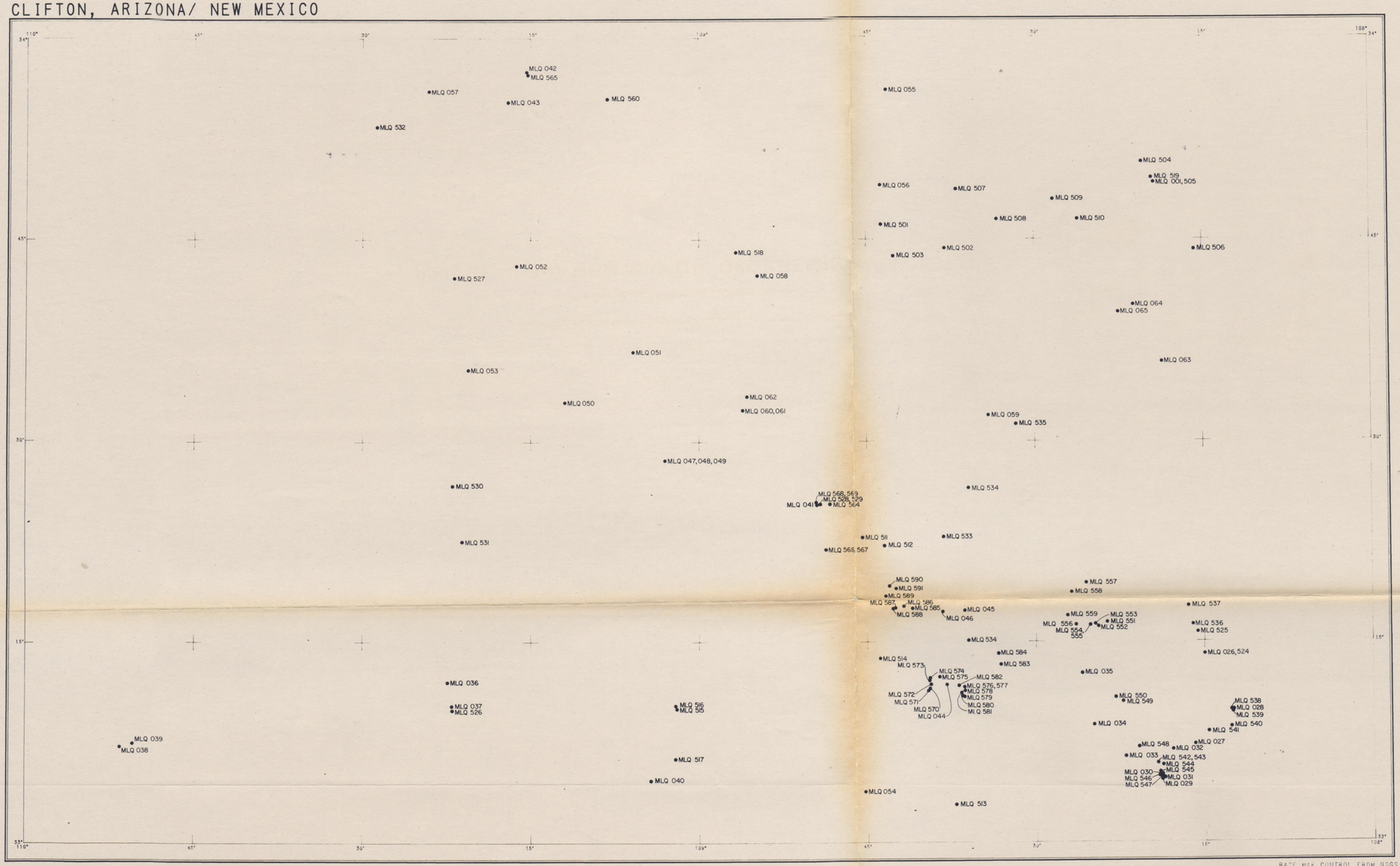

URANIUM RESOURCE EVALUATION
ISSUED BY THE U.S. DEPARTMENT OF ENERGY

5 0 5 10 15 20 25 MILES

5 0 5 10 15 20 25 KILOMETERS

BASE MAP CONTROL FROM USGS

Plate 5a. LOCATION MAP OF GEOCHEMICAL SAMPLES

February 1981
Plate 5a.

CLIFTON, ARIZONA/ NEW MEXICO

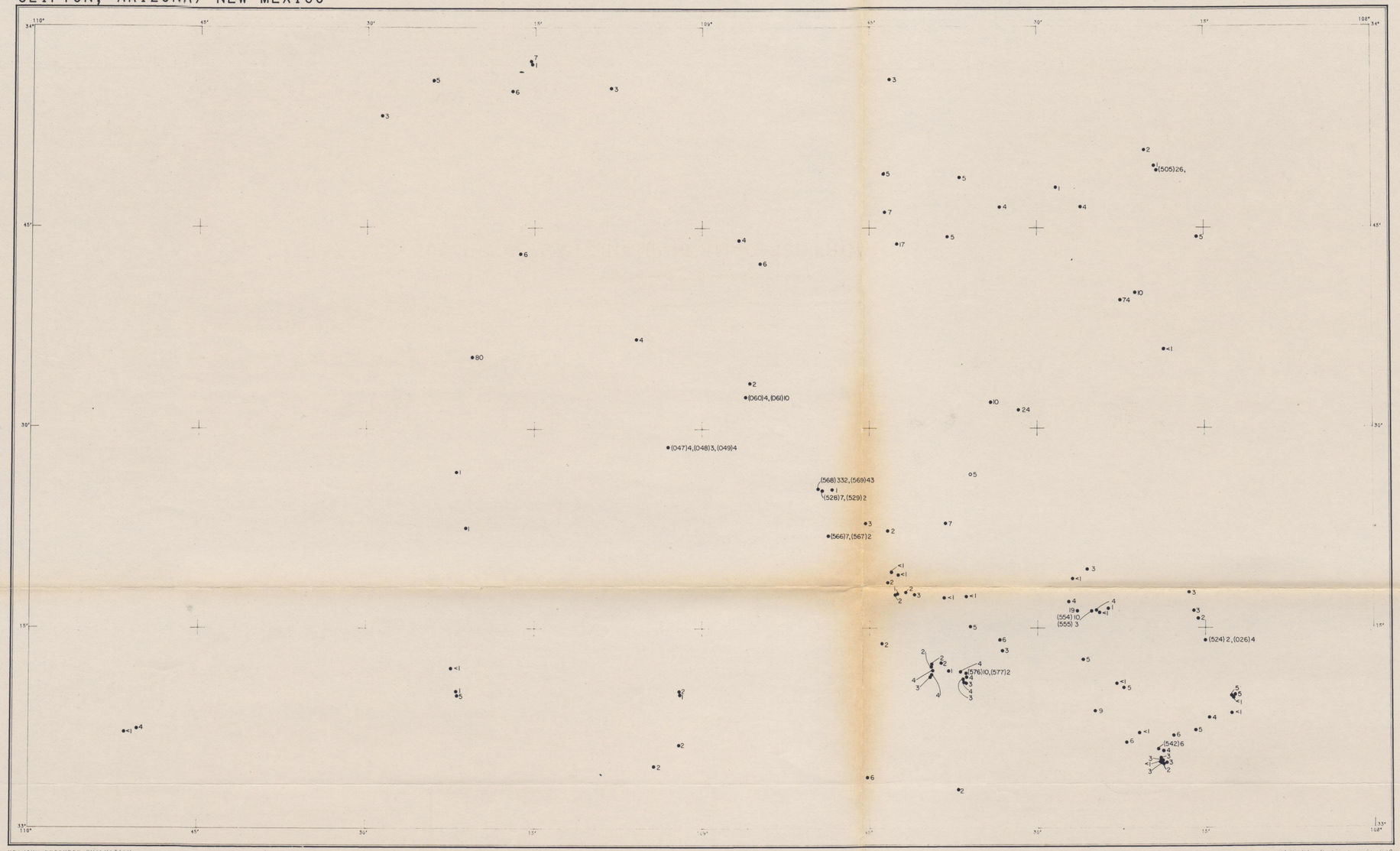

EXPLANATION

- • Sample location
- (Sample number)
- 6 Parts per million chemical uranium

URANIUM RESOURCE EVALUATION
ISSUED BY THE U.S. DEPARTMENT OF ENERGY

BASE MAP SOURCE: USGS, INC.

5 0 5 10 15 20 25 MILES

5 0 5 10 15 20 25 KILOMETERS

Plate 5b. RESULTS OF URANIUM ANALYSES FROM ROCK SAMPLES

February 1981
Plate 5b.

5 0 5 10 15 20 25 MILES

5 0 5 10 15 20 25 KILOMETERS

URANIUM RESOURCE EVALUATION
ISSUED BY THE U.S. DEPARTMENT OF ENERGY

BASE MAP CONTROL FROM USGS

Plate 6. DRAINAGE

CLIFTON, ARIZONA/ NEW MEXICO

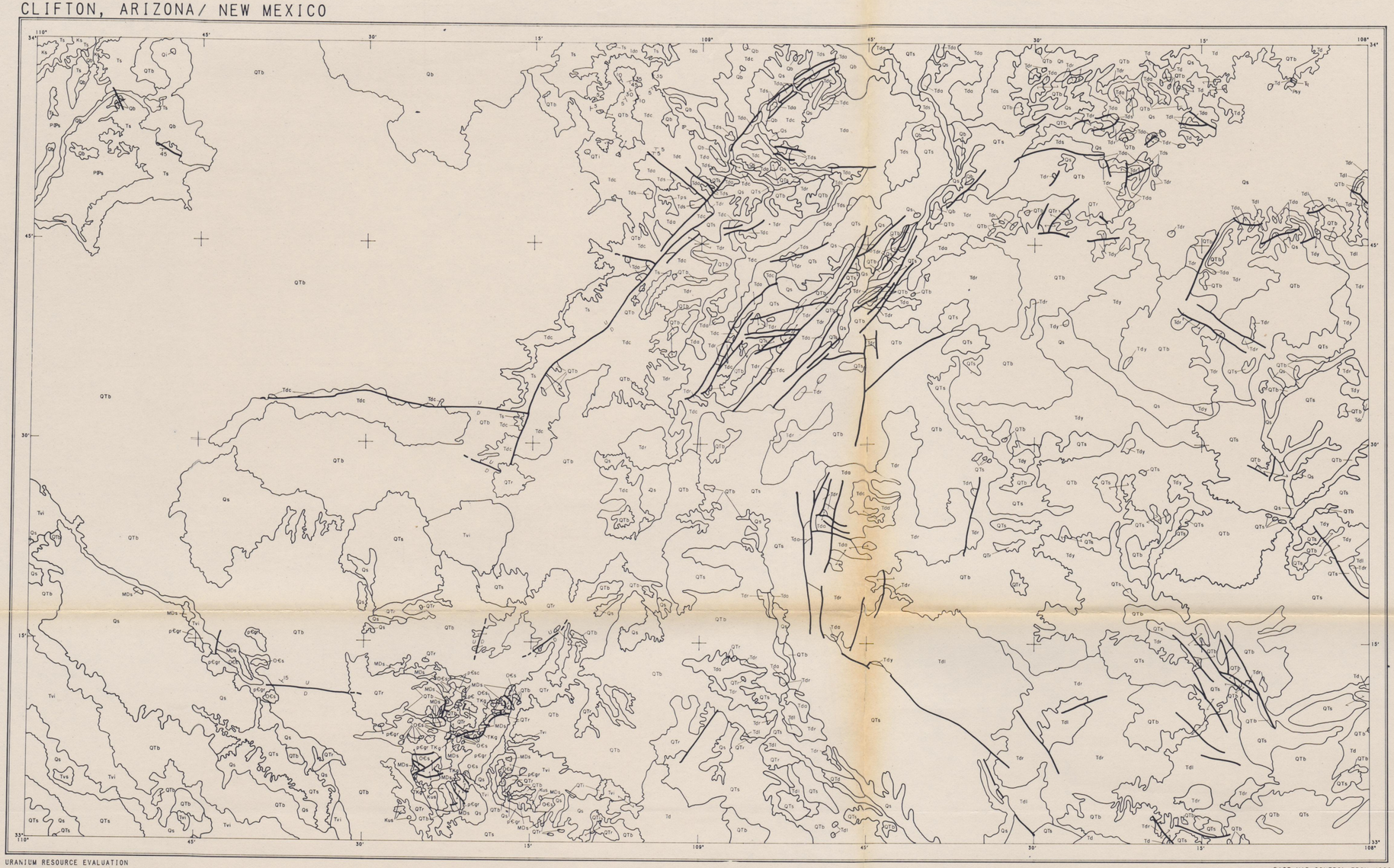

URANIUM RESOURCE EVALUATION
ISSUED BY THE U.S. DEPARTMENT OF ENERGY

5 0 5 10 15 20 25 MILES

5 0 5 10 15 20 25 KILOMETERS

BASE MAP CONTROL FROM USGS
DATA SOURCE: QUAHADA ENGINEERING, MODIFIED BY D.L. WHITE AND S.L. REED.

Plate 7. GEOLOGIC MAP

1955 MAGNETIC DECLINATION FOR THIS SHEET VARIES FROM 13° 30' EASTERLY FOR THE CENTER OF THE WEST EDGE TO 13°00' EASTERLY FOR THE CENTER OF THE EAST EDGE. MEAN ANNUAL CHANGE IS 0° 02' WESTERLY.

DATA SOURCE MAP

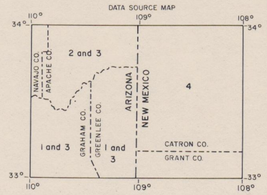

EXPLANATION

Qs — Sedimentary deposits
Mainly alluvial gravel, sand and silt in flood plains, terraces, fans and pediment coppings. Locally includes dune sand, lake deposits and landslide masses. Shown only in areas where they are of appreciable thickness or extent.

QTs — Sedimentary deposits
Includes Gila Conglomerate and other stream and lake deposits mainly in intermontane areas. Consists of loosely to firmly consolidated gravel, sand, silt, local clay, gypsum, marl, limestone, diatomite and some intercalated basalt flows and felsic tuff beds.

Ts — Sedimentary rocks
Mainly conglomerate, sandstone, siltstone, limestone and tuffaceous beds. Locally may include volcanic units ranging from rhyolite to andesite.

Ks **Kus** — Sedimentary rocks
Ks, includes Amole Arkose and Recreation Red Beds of Brown (1939) and other units of known or supposed Cretaceous age.
Kus, includes Pinkard Formation in Greenlee County and probably equivalent beds in Graham County.

Pc — Coconino Sandstone

Psy — San Andres Limestone and Yeso Formation, undivided (Glorieta Sandstone not present)

PSPs — Supai Formation

MDs — Sedimentary rocks
Includes Upper Mississippian Paradise Formation of Stoyanow (1926) and Hermon (1935), Modoc Limestone (Lower Mississippian) and Morenci Shale (Upper Devonian), and locally Pennsylvanian Limestone.

OCs — Sedimentary rocks
Includes Longfellow Limestone (Lower Ordovician and Upper Cambrian) and Coronado Quartzite (Upper Cambrian) in Greenlee County.

pCsc — Pinal Schist

Qb **Qi** — Volcanic rocks
Qb, basaltic flows, agglomerate, tuffs and cinders distinguished from older basalts. Locally includes trachyte, latite, andesite and also some intrusive rocks. May include some flows of Pliocene age.
Qi, dikes and plugs, mainly basaltic in composition.

QTb **QTi** **QTr** — Volcanic rocks
Includes some interfingering with QTs and older units whose debris is in QTs.
QTb, basalt flows, agglomerate, tuff and cinders.
QTi, dikes and plugs, mainly andesitic to basaltic in composition.
QTr, rhyolite flows and pyroclastic rocks.

Ti **Tvi** **Tvs** — Volcanic rocks
Flows, tuffs, breccias and agglomerates interfingering with Tertiary sediments in part. Includes some dikes and plugs.
Ti, dikes, sills and plugs, rhyolitic to basaltic in composition.
Tvi, intermediate volcanic rocks.
Tvs, silicic volcanic rocks.

Tdy **Tdo** **Tdl** **Td** **Tds** **Tdc** **Tdr** — Datil Formation
Td, where undivided comprises a sequence that may be divided into facies which are locally superimposed units as follows:
Tdy, rhyolite flows with phenocrysts of sanidine and smoky quartz.
Tdo, andesite and basaltic andesite flows and intrusive rocks.
Tds, clastic rocks of volcanic fragments.
Tdc, boulder beds and coarse conglomerates chiefly of volcanic fragments and correlative sand, silt and clay deposited in the valleys of the present drainage systems.
Tdr, welded and crystal rhyolite tuffs, flows and breccias.
Tdl, latite breccias, flow-banded latite with andesite and rhyolite.

TKg — Intrusive rocks
Granite, quartz monzonite, granodiorite, quartz diorite and some porphyritic equivalents.

Tr — Triassic rocks, undivided

IP — Pennsylvanian rocks, undivided

pCgr — Intrusive rocks
Granite, quartz monzonite, granodiorite and quartz diorite.

CENOZOIC — QUATERNARY; TERTIARY
MESOZOIC — CRETACEOUS; TRIASSIC
PALEOZOIC — PERMIAN; DEVONIAN, PENNSYLVANIAN, MISSISSIPPIAN; CAMBRIAN, ORDOVICIAN
PROTEROZOIC — PRECAMBRIAN

GEOLOGIC SYMBOLS
- Formation contact
- Fault — Dotted where concealed, dashed where inferred, D, downthrown side
- Anticline
- Dip and strike

DATA SOURCES

1. Geologic map of Graham and Greenlee Counties, Arizona. Arizona Bureau of Mines, Tucson, Arizona. Eldred D. Wilson and Richard T. Moore, with additional data from maps by W. Lindgren, J.M. Boutwell, J.R. Cooper and C.S. Bromfield, U.S. Geological Survey. Basic materials furnished by U.S. Geological Survey. 1:375,000 scale. 1959.

2. Geologic map of Navajo and Apache Counties, Arizona. Arizona Bureau of Mines, Tucson, Arizona. Eldred D. Wilson, Richard T. Moore, Eldred D. Wilson and Robert T. O'Hare. 1:375,000 scale. 1960.

3. Geologic map of Arizona. Arizona Bureau of Mines and the U.S. Geological Survey. Eldred D. Wilson and Richard T. Moore, Arizona Bureau of Mines and John R. Cooper, U.S. Geological Survey. 1:500,000 scale. 1969.

4. Geologic map of New Mexico. Department of the Interior, U.S. Geological Survey, New Mexico Institute of Mining and Technology, State Bureau of Mines and Mineral Resources Division and the University of New Mexico, Department of Geology. Corle H. Dane and George O. Bachman. 1:500,000 scale. 1965.

February 1981
Plate 7.

CLIFTON, ARIZONA/ NEW MEXICO

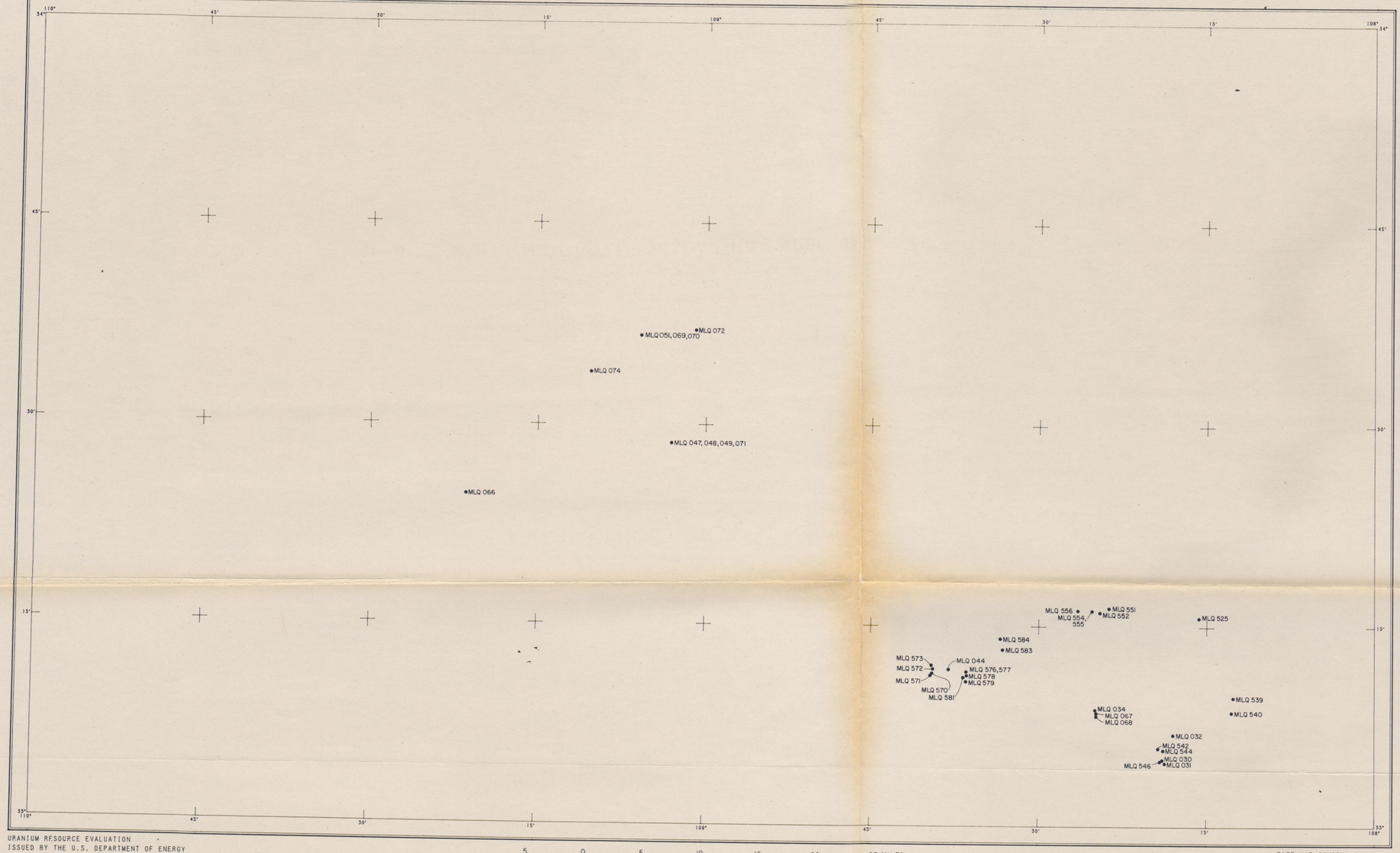

URANIUM RESOURCE EVALUATION
ISSUED BY THE U.S. DEPARTMENT OF ENERGY

5 0 5 10 15 20 25 MILES

5 0 5 10 15 20 25 KILOMETERS

BASE MAP CONTROL FROM USGS

Plate 8. LOCATION OF FIELD GAMMA-RAY SPECTROMETRY SAMPLES

February 1981

Plate 8.

CLIFTON, ARIZONA/ NEW MEXICO

EXPLANATION

- Boundary of caldera or volcano-tectonic depression
- Fault, dashed where approximate; ball and bar indicates down-dropped side
- Approximate limit of inferred pluton
- Approximate boundary of Mogollon Plateau

DATA SOURCES: ELSTON AND OTHERS, 1976; RATTÉ AND OTHERS, 1979; RHODES, 1976b.

LOCATION MAP

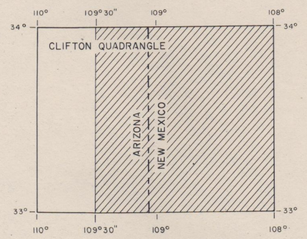

TRUE NORTH

MAGNETIC NORTH

Plate 9. LOCATION OF KNOWN CALDERAS

February 1981

Plate 9.

CLIFTON, ARIZONA/ NEW MEXICO

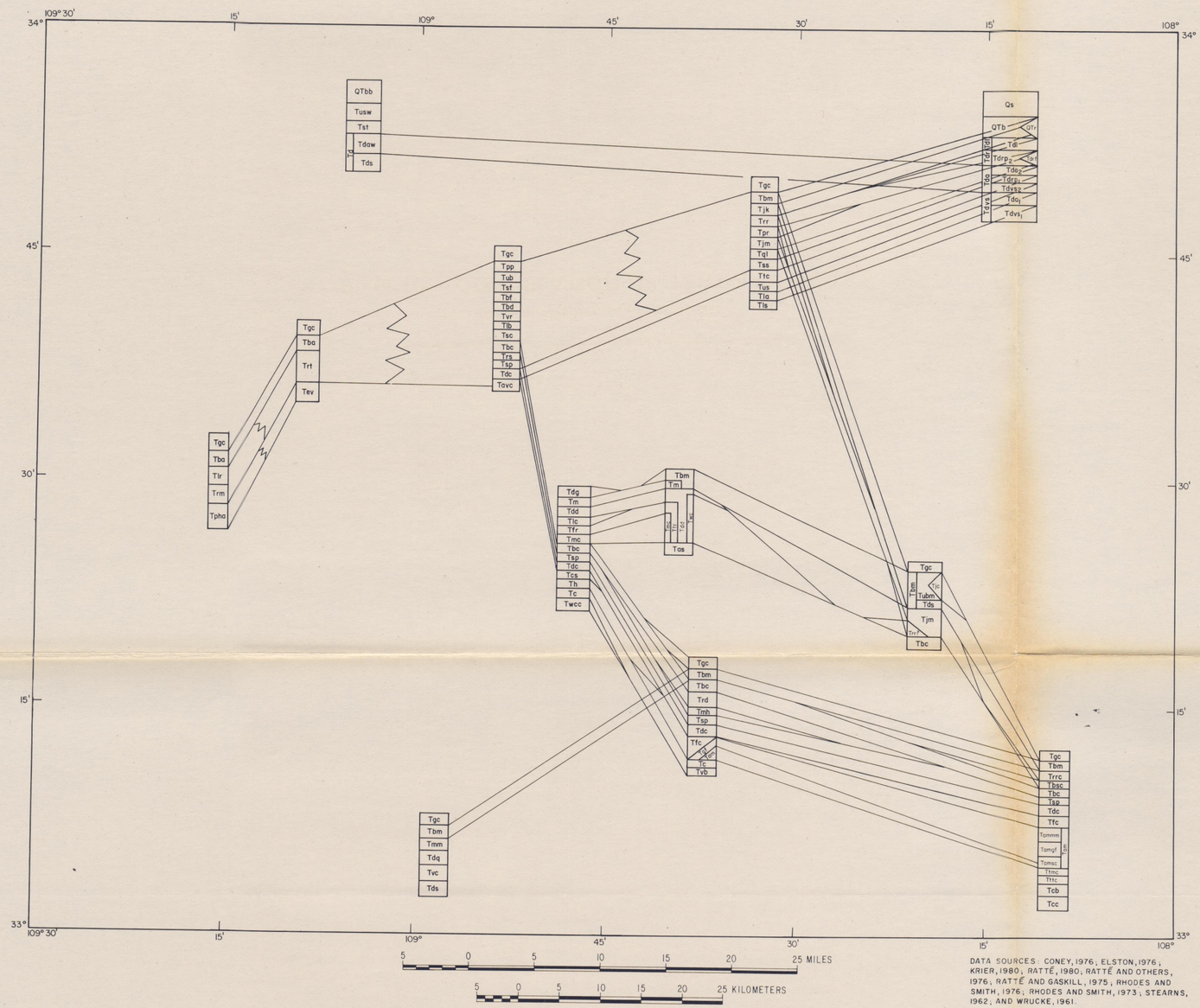

DATA SOURCES: CONEY, 1976; ELSTON, 1976; KRIER, 1980; RATTÉ, 1980; RATTÉ AND OTHERS, 1976; RATTÉ AND GASKILL, 1975; RHODES AND SMITH, 1976; RHODES AND SMITH, 1973; STEARNS, 1962; AND WRUCKE, 1961.

Plate 10. CORRELATION OF TERTIARY UNITS

TRUE NORTH

MAGNETIC NORTH

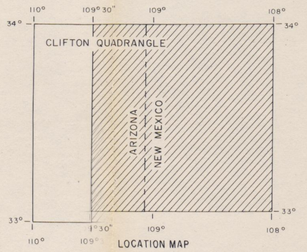

LEGEND

- **Qs** Sedimentary deposits—Quaternary—includes littoral deposits of San Agustin, landslide debris, alluvium, and bolson deposits
- **QTb** Basalt, andesite, and latite flows of Stearns (1962)—Tertiary-Quaternary
- **QTbb** Local basalt flows of Wrucke (1961)—Tertiary-Quaternary
- **Tgc** Gila Conglomerate—Miocene-Pleistocene—fanglomerate—conglomerate and sandstone with local basalt flows. Ages range from 20.6 ±1.5 m.y. of a basal andesite in the Gila Valley, to 0.9 ±0.2 m.y. of a basalt near the top of the formation at Apache Creek
- **Tdg** Dog Gulch Formation—Miocene—conglomerate
- **Tbm** Bearwallow Mountain Formation—Miocene—basalt, basaltic andesite, andesite, and latite flows
- **Tds** Double Springs Andesite—Miocene—basaltic andesite
- **Tm** Mogollon Andesite—Miocene (17.1 ±0.3 m.y.)—andesite to latite. May be equivalent to the Double Springs Andesite
- **Tmm** Mule Mountain Rhyolite—Miocene (18.6 m.y.)—crystal-poor, flow-banded rhyolite
- **Tvs** Volcaniclastic sediments—Miocene—pumice and ash-fall deposits
- **Tds** Dripping Springs Formation—Miocene—mudflow breccia overlain by ash-flow tuff
- **Tpp** Basalt of Pueblo Park—Miocene (19.2 ±2.5 m.y.)—olivine basalt flows. Correlates with upper basalt along the San Francisco River
- **Tub** Upper basalt along San Francisco River—Miocene—basalt flows. Correlates with Basalt of Pueblo Park
- **Tusw** Upper Sedimentary Formation of Wrucke (1961)—Miocene (?)—basal fluvial sandstone overlain by eolian sandstone
- **Tsf** Basaltic breccia along San Francisco River and cinder cones of lower Saliz Canyon and Bang Trail Canyon—Miocene
- **Tdq** Domes and flows of quartz latite and rhyolite of Rhodes and Smith (1973)—Miocene
- **Tjk** John Kerr Peak Formation—Miocene (21.4 ±1.1 m.y.)—quartz latite domes and lava flows. correlates with QTr of Stearns (1962)
- **QTr** Rhyolite flows of Stearns (1962)—correlates with the John Kerr Peak Formation
- **Tjc** Jordan Canyon Formation—Miocene (21.7 ±0.7 m.y.)—sandstone and air-fall tuff grading up into breccia and sandstone-conglomerate
- **Tdd** Deadwood Gulch Formation—Miocene—interbedded tuff, sandstone, and conglomerate
- **Trrc** Rhyolite of Rocky Canyon—Miocene—flow-banded rhyolitic flows and domes
- **Trr** Railroad Canyon Tuff—Oligocene-Miocene (27.4 ±0.9 m.y.)—crystal-rich, ash-flow tuff. Correlates with upper part of $Tdrp_2$ of Stearns (1962)
- **Tpr** Pumiceous rhyolitic tuff of Rhodes and Smith (1976)—Oligocene-Miocene—similar appearance to the Deadwood Gulch Formation
- **Tjm** Jerky Mountain Rhyolite—Oligocene-Miocene—massive, flow-banded, rhyolitic lava. Correlates with Tdrf of Stearns (1962)
- **Tba** Basaltic andesite of Ratté (1969)—Oligocene-Miocene (23.3 ±0.7 m.y.)
- **Tlr** Quartz latite and rhyolite complex of Ratté (1969)—Oligocene-Miocene (23.4 ±0.7 m.y.)—extrusive-intrusive dome complex, dikes intrude lower basaltic andesite
- **Trm** Rhyolite of Red Mountain—Oligocene-Miocene—welded ash-flow tuffs, lava flows, and intrusive rhyolite
- **Trt** Rhyolite tuff of Ratté (1969)—Oligocene-Miocene (24.9 ±0.7 m.y.)—ash-flow tuff interlayered with conglomerate, sandstone, and andesitic lava flows
- **Tlc** Last Chance Andesite—Oligocene-Miocene (25.0 ±0.5 m.y.)—variable andesite flows interbedded with breccia and sandstone
- **Tbf** Basalt and andesite flows of Ratté (1980)—Oligocene(?)-Miocene
- **Tbd** Basalt or andesite dikes of Ratté (1980)—Oligocene(?)-Miocene—may be related to Basalt of Pueblo Park
- **Tvr** Volcaniclastic rocks of Ratté (1980)—Oligocene(?)-Miocene—fanglomerate interlayered with volcanic rocks
- **Tlb** Lower basalt flows of Ratté (1980)—Oligocene(?)-Miocene—includes basalt of Saliz Hill
- **Tsc** Andesitic intrusion of Saliz Canyon—Oligocene(?)-Miocene
- **Tfr** Fanney Rhyolite—Oligocene-Miocene (27.6 m.y.)—flow-banded lava interlayered with flow breccia and tuff
- **Tmc** Mineral Creek Andesite—Oligocene-Miocene
- **Twc** Porphyritic latite of Willow Creek—Oligocene-Miocene—equivalent to Sacaton Mountain Quartz Latite and porphyritic latite of Negrito Creek
- **Tas** Apache Spring Quartz Latite—Oligocene-Miocene (27.3 ±0.8 m.y.)—porphyritic, ash-flow tuff
- **Tql** Quartz latite ash-flow tuff of Rhodes and Smith (1976)—Oligocene-Miocene—correlates with $Tdrp_2$ of Stearns (1962). May correlate with Apache Spring Quartz Latite
- **Tbc** Bloodgood Canyon Tuff—Oligocene(?) (27.4 ±3.4 m.y.)—rhyolitic, phenocryst-rich, ash-flow tuff
- **Trd** Rhyolite of Diablo Range—Oligocene(?) (27.6 ±4.5 m.y.)—flow-banded domes and flows with pyroclastic or volcanistic facies and a welded-tuff facies
- **Trs** Red sandstone unit of Ratte (1980)—Oligocene
- **Tst** Siltstone and tuff unit of Wrucke (1961)—mid-Eocene(?)-Miocene(?)
- **Tmh** Andesite flows and breccias of Murtock's Hole—Oligocene(?)
- **Tss** Squirrel Springs Canyon Andesite—Oligocene—correlates with Tda_2 of Stearns (1962)
- **Tsp** Tuff of Shelly Peak—Oligocene (29.0 ±1.0 m.y.)—compositionally zoned, phenocryst-rich, ash-flow tuff
- **Tdc** Tuff of Davis Canyon—Oligocene (30.7 ±1.0 m.y.)—crystal-poor, rhyolitic ash-flow tuff
- **Ttc** Tularosa Canyon Rhyolite—Oligocene (30.7 ±1.3 m.y.)—ash-flow tuff, overlain by tuffaceous sandstone. Correlates with $Tdrp_1$ of Stearns (1962) and tuff of Davis Canyon
- **Tfc** Tuff of Fall Canyon—Oligocene—rhyolitic or quartz latitic ash-flow tuff
- **Tus** Upper sedimentary unit of Rhodes and Smith (1976)—Oligocene—interbedded sandstone, gravel, and mudflow breccia. correlates with $Tdvs_2$ of Stearns (1962)
- **Tla** Lower andesite unit of Rhodes and Smith (1976)—Oligocene—correlates with Tda_1 of Stearns (1962)
- **Tls** Lower sedimentary unit of Rhodes and Smith (1976)—Oligocene—bedded sandstone, conglomerate, and mudflow breccia. Correlates with $Tdvs_1$ of Stearns (1962)
- **Td** Datil Formation of Stearns (1962)—Tertiary
  - **Tdl** Latite facies—latite with upper and lower flow breccia
  - **Tdr** Rhyolite facies
    - **Tdrf** Correlates with Jerky Mountain Rhyolite
    - **$Tdrp_1$** Interbedded tuff, tuff breccia, sandstone, siltstone, and clay
    - **$Tdrp_2$** Correlates with quartz latite ash-flow tuff of Rhodes and Smith (1976). Upper part correlates with Railroad Canyon Tuff
  - **Tda** Andesite facies—correlates with andesite member of Wrucke (1961)
    - **Tda_1** Correlates with lower andesite of Rhodes and Smith (1976)
    - **Tda_2** Correlates with Squirrel Springs Canyon Andesite
  - **Tdvs** Volcanic sedimentary facies
    - **$Tdvs_1$** Correlates with lower sedimentary unit of Rhodes and Smith (1976)
    - **$Tdvs_2$** Correlates with upper sedimentary unit of Rhodes and Smith (1976)
    - **$Tdvs_3$** Tuffaceous sandstone
  - **Tdaw** Andesite member of Datil Formation of Wrucke (1961). Correlates with Tda of Stearns (1962)
  - **Tds** Sedimentary member of Datil Formation of Wrucke (1961). Correlates with Tda of Stearns (1962)
- **Tgf** Latite and andesitic lava flows of Gila Flat—Oligocene (29.6±1.0 m.y.)
- **Tcs** Cranktown Sandstone—Oligocene—volcaniclastic sandstone
- **Th** Houston Formation—Oligocene—andesite flow. correlates with Alum Mountain Formation
- **Tam** Alum Mountain Formation—Oligocene. Correlates with Houston Formation
  - **Tammm** Middle Mountain Member—andesite
  - **Tamgf** Gila Flat Member (30.5±1.0 m.y.)—andesite flows and breccias
  - **Tamsc** Salt Creek Member (30.5±1.0 m.y.)
- **Ttmc** Tuff of Monument Canyon—Oligocene—rhyolitic or quartz latitic tuff
- **Ttfc** Tuff of Terry Canyon—Oligocene—crystal-rich tuff
- **Tcb** Caballo Blanco Rhyolite Tuff—Oligocene (30.2 ±0.8 m.y.)—crystal-rich, ash-flow tuff
- **Tc** Cooney Quartz Latite—Oligocene (32.5 ±1.5 m.y.)—compositionally zoned, ash-flow tuff. Lower member is the Whitewater Creek Rhyolite
- **Twcc** Whitewater Creek Rhyolite—Oligocene—ash-flow tuff and rhyolite domes
- **Tvb** Volcanic complex of Brock Canyon—Oligocene (30-34 m.y.)—fresh to intensely altered latitic to andesitic lava flows and flow breccia
- **Tavc** Early andesitic volcanic complex—Oligocene (33.1 ±2.7 m.y.)—andesitic to intermediate composition vent facies, volcaniclastic breccias, tuffs, and flows
- **Tcc** Andesite of Turkey Cienega Canyon—Oligocene or older—andesitic flows and breccias
- **Tpha** Pyroxene-hornblende andesite of Ratté (1969)—Eocene-Oligocene—(37.4 ±3.9 m.y.)—lava flows, flow breccias, and pyroclastic breccias
- **Tev** Epiclastic volcanic rocks—Eocene-Oligocene—interbedded nonvolcanic conglomerate and andesitic to dacitic lava flows

CLIFTON, ARIZONA/ NEW MEXICO

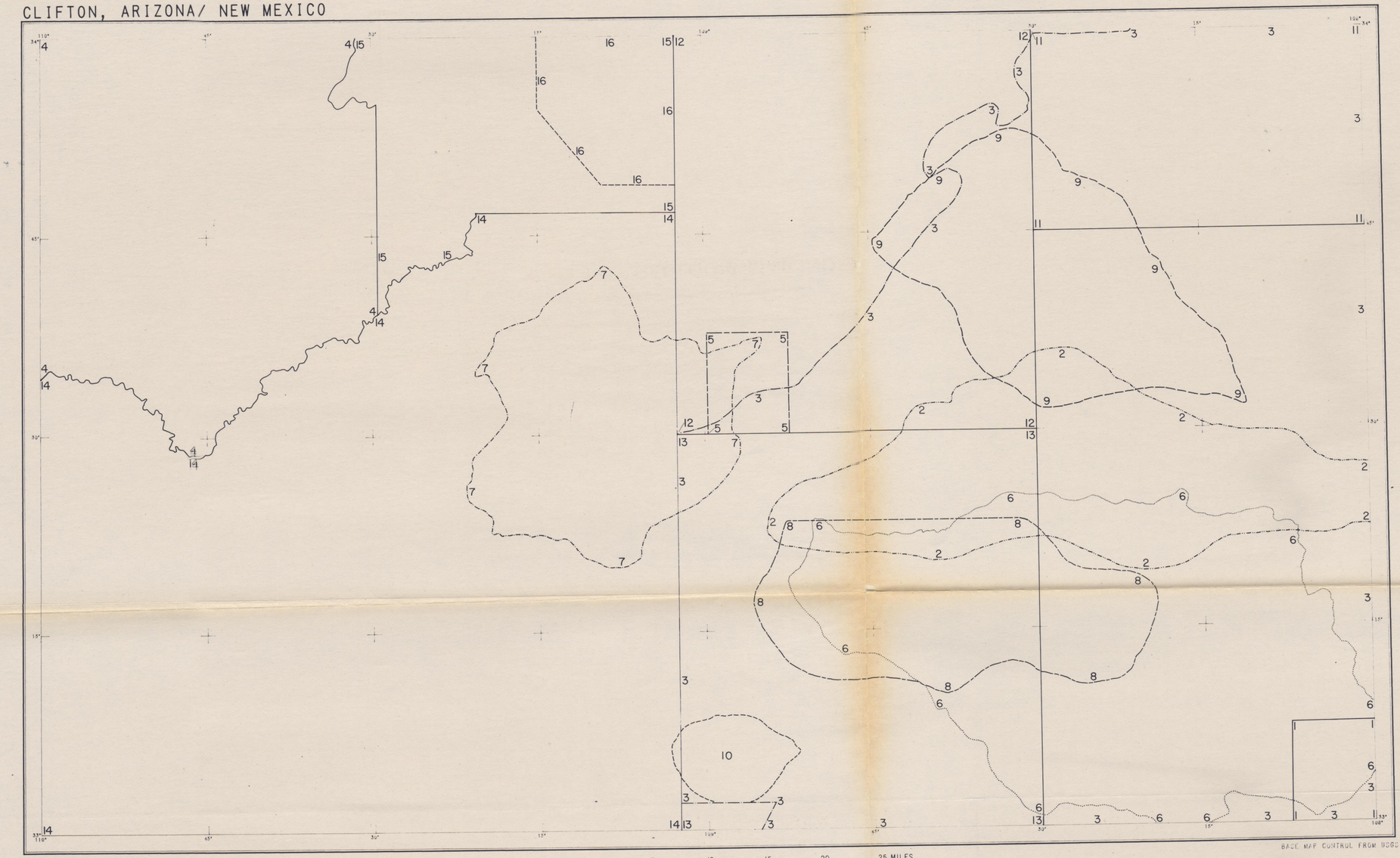

INDEX

1. Aldrich, 1976, scale 1:24,000.
2. Coney, 1976, scale 1:126,720.
3. Elston and others, 1976, scale 1:320,800.
4. Moore, 1968, scale 1:230,000.
5. Ratté, 1980, scale 1:24,000.
6. Ratté and Gaskill, 1975, scale 1:62,500.
7. Ratté, Lands, and Gaskill, 1969, scale 1:62,500.
8. Rhodes, 1976, scale 1:160,000.
9. Rhodes and Smith, 1976, scale 1:110,000.
10. Rhodes and Smith, 1973, scale 1:63,300.
11. Stearns, 1962, scale 1:63,360.
12. Weber and Willard, 1959a, scale 1:126,720.
13. Weber and Willard, 1959b, scale 1:128,720.
14. Wilson and Moore, 1958, scale 1:375,000.
15. Wilson, Moore, and O'Maire, 1960, scale 1:126,720.
16. Wrucke, 1961, scale 1:62,500.

URANIUM RESOURCE EVALUATION
ISSUED BY THE U.S. DEPARTMENT OF ENERGY

5 0 5 10 15 20 25 MILES

5 0 5 10 15 20 25 KILOMETERS

BASE MAP CONTROL FROM USGS

Plate 11. GEOLOGIC-MAP INDEX

February 1981
Plate 11.

CLIFTON, ARIZONA/ NEW MEXICO

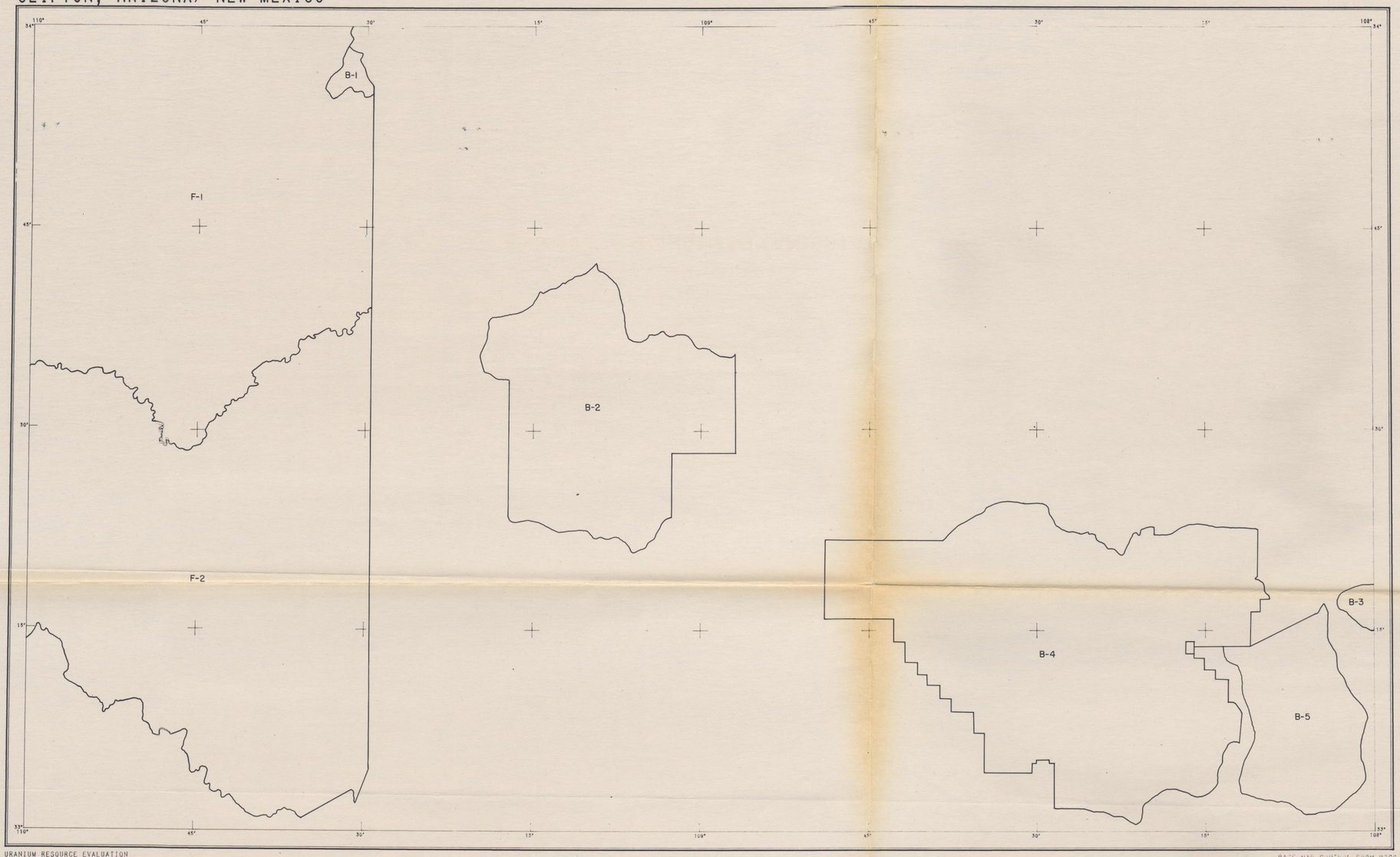

URANIUM RESOURCE EVALUATION
ISSUED BY THE U.S. DEPARTMENT OF ENERGY

5 0 5 10 15 20 25 MILES

5 0 5 10 15 20 25 KILOMETERS

BASE MAP CONTROL FROM USGS

INDEX

B. Forest Service Wilderness, Wilderness Study, and Primitive Areas

- B-1 Mt. Baldy Wilderness Area
- B-2 Blue Ridge Primitive Area
- B-3 Black Range Primitive Area
- B-4 Gila Wilderness
- B-5 Gila Primitive Area

F. Indian Lands

- F-1 Fort Apache Indian Reservation
- F-2 San Carlos Indian Reservation

Plate 12. GENERALIZED LAND STATUS

February 1981
Plate 12.

CLIFTON, ARIZONA/ NEW MEXICO

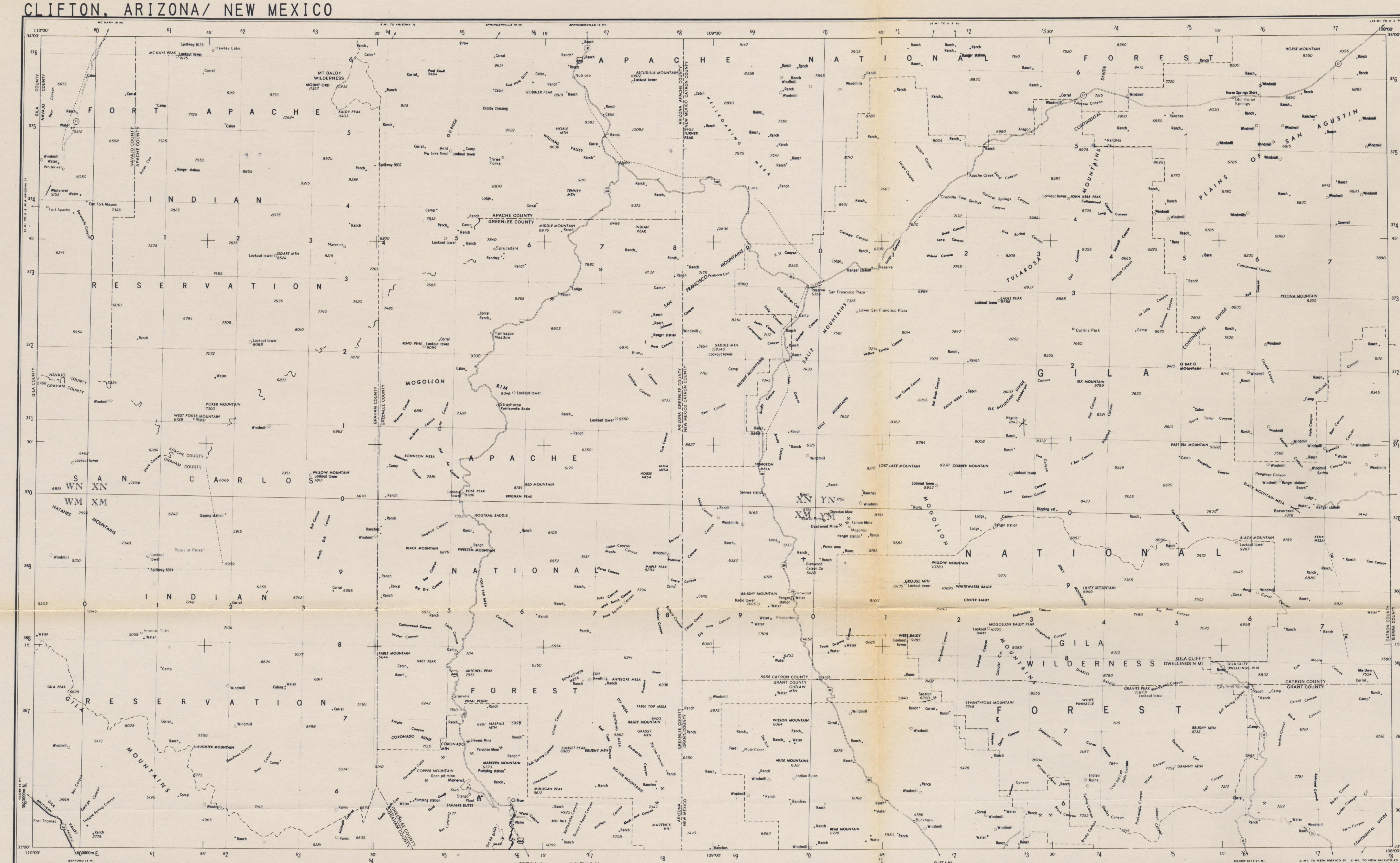

URANIUM RESOURCE EVALUATION
ISSUED BY THE U.S. DEPARTMENT OF ENERGY

BASE MAP CONTROL FROM USGS

5 0 5 10 15 20 25 MILES

5 0 5 10 15 20 25 KILOMETERS

Plate 13. CULTURE

February 1981

Plate 13.

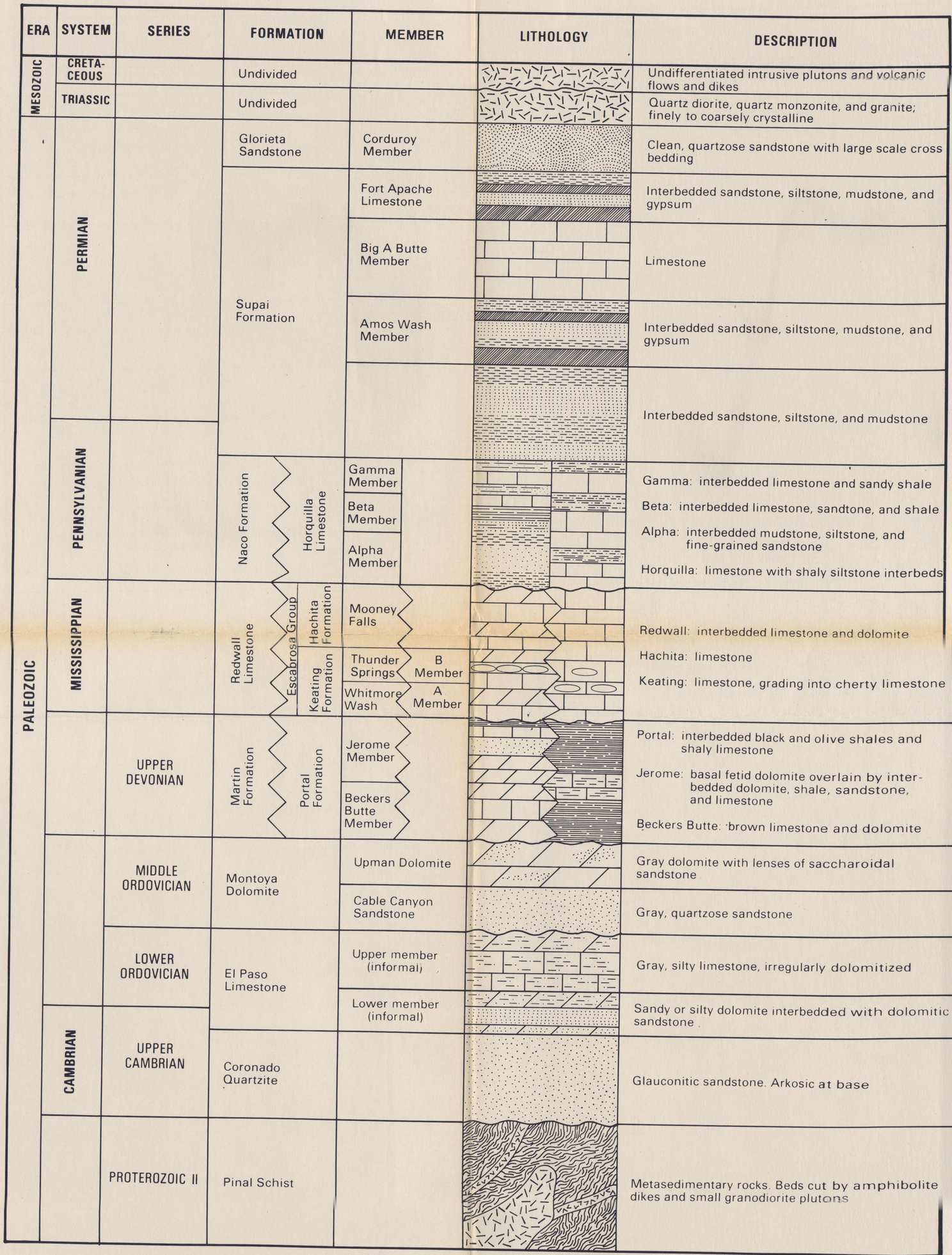

Figure 3a. Generalized stratigraphic column of pre-Tertiary rocks in the Arizona portion of the Clifton Quadrangle.

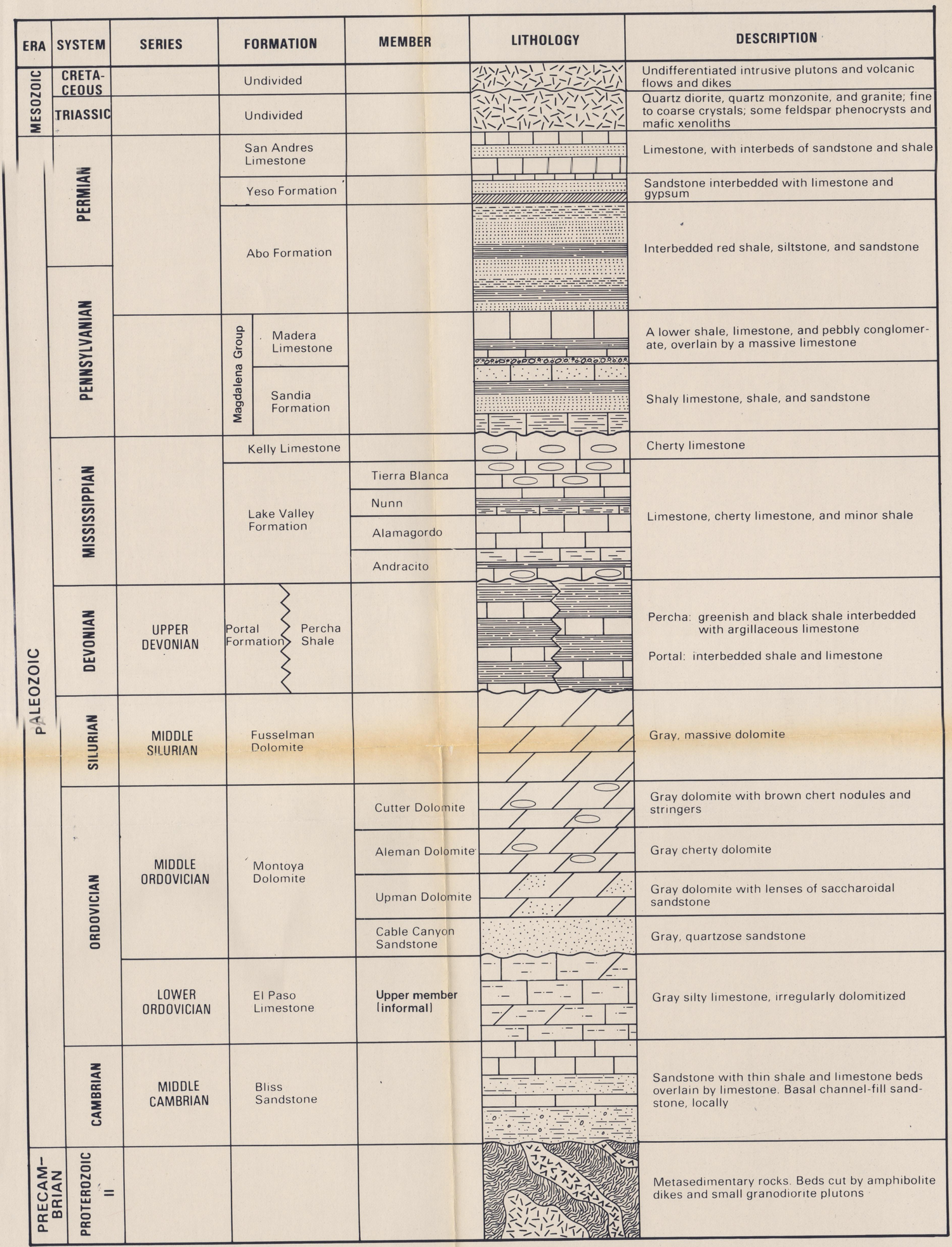

Figure 3b. Generalized stratigraphic column of pre-Tertiary rocks in the New Mexico portion of the Clifton Quadrangle.

SYSTEM	SERIES	FORMATION	MEMBER	LITHOLOGY	DESCRIPTION
CENOZOIC	PLIOCENE-PLEISTOCENE	Gila Conglomerate			Terrace gravel, pediment gravel; bolson deposits, morainal deposits, basalt flows, and alluvium
		Bearwallow Mountain, Gila Flat, Murtock's Hole	Basaltic Andesite		Olivine alkali basalt, interlayered with Gila Conglomerate; some cinder cones and lake deposits
	MIOCENE				Dark-colored flows of predominantly basaltic-andesitic composition; ranges from basaltic to quartz latitic composition
	OLIGOCENE-MIOCENE	Apache Springs Quartz Latite, Bloodgood Canyon Rhyolite Tuff, Tuff of Fall Canyon, Tularosa Canyon Rhyolite Tuff, John Kerr Peak Quartz Latite, Quartz Latite of Nabors Mountain, Sacaton Quartz Latite, Jordan Canyon, Fanny Rhyolite, Jerky Mountain Rhyolite, Mule Mountain Rhyolite, Tuff of Diablo Mts., Willow Creek, Negrito Creek	High-Silica Alkali-Rhyolite Suite		Ash-flow tuff deposits of rhyolitic composition
					Highly porphyritic flows and domes of flow-banded rhyolite and quartz latite; primarily cauldron lavas
					Sparsely porphyritic flows and domes of flow-banded rhyolite with local pumice beds; mainly framework lavas and moat deposits
					Pumiceous flows, interlayered ash-flow tuff, conglomerate and landslide debris; mainly moat deposits
	OLIGOCENE	Railroad Canyon Tuff, Tuff of Davis Canyon Tuff of Shelly Peak, Alum Mountain, Dripping Spring, Last Chance Andesite, Mineral Creek Andesite, Holt Gulch, Squirrel Springs Canyon Andesite, Whitewater Creek Rhyolite, Cooney Qurtz Latite, Turkey Cienega Canyon	Calc-Alkalic Suite		Ash-flow tuff of rhyolitic composition
					Dark-colored flows, predominantly andesite; ranges from basaltic to quartz latitic composition
					Ash-flow tuff ranging from quartz latitic to rhyolitic compositions
					Porphyritic flows and domes; rhyolitic to quartz latitic composition; mainly cauldron lavas
					Domes and flows of porphyritic rhyolite; mainly ring-fracture domes
	EOCENE - EARLY OLIGOCENE	Brock Canyon			Pumiceous flows; tuffaceous sandstone and conglomerate; ash-flow tuff; mostly moat deposits
		Baca			Interbedded red, purple, yellow, arkosic sand stone, conglomerate, shale, and mudstone

* Favorable for uranium deposition

Figure 3c. Generalized stratigraphic column of Tertiary rocks in the Clifton Quadrangle.

CLIFTON, ARIZONA/ NEW MEXICO

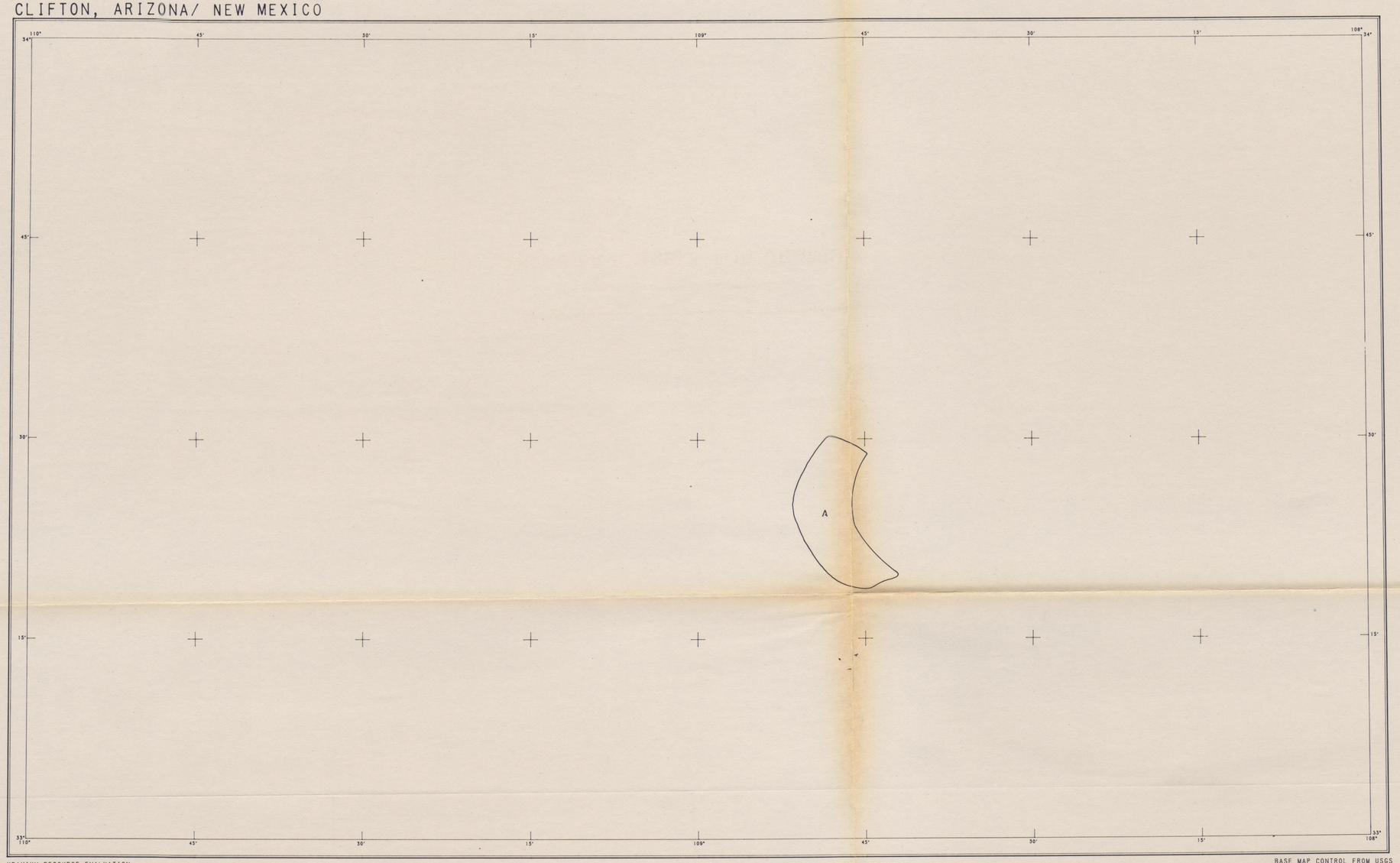

EXPLANATION

Favorable areas

URANIUM RESOURCE EVALUATION
ISSUED BY THE U.S. DEPARTMENT OF ENERGY

5 0 5 10 15 20 25 MILES

5 0 5 10 15 20 25 KILOMETERS

BASE MAP CONTROL FROM USGS

Plate 1. AREAS FAVORABLE FOR URANIUM DEPOSITS

February 1981
Plate 1.